NASA Contractor Report 3069

Feasibility of Combining Linear Theory and Impact Theory Methods for the Analysis and Design of High Speed Configurations

D. Brooke and D. V. Vondrasek

NASA

NASA Contractor Report 3069

Feasibility of Combining Linear Theory and Impact Theory Methods for the Analysis and Design of High Speed Configurations

D. Brooke and D. V. Vondrasek
McDonnell Douglas Corporation
St. Louis, Missouri

NASA

National Aeronautics
and Space Administration

**Scientific and Technical
Information Office**

1979

TABLE OF CONTENTS

LIST OF ILLUSTRATIONS

SUMMARY

This investigation examined the feasibility of combining elements of linear theory and impact theory to provide improved aerodynamic predictions for the analysis and design of high speed configurations in the Mach 4 to 8 range. Specifically, the aerodynamic influence coefficients calculated using an existing linear theory program were used to modify the pressures calculated using impact theory. This combined approach was used to calculate local pressures and loadings over several wing-alone configurations. Comparisons with experimental pressure data show that the combined approach gives improved predictions over either linear theory alone or impact theory alone. The results of the study show that the combination of linear theory and impact theory not only removes most of the shortcomings of the individual methods as applied in the Mach 4 to 8 range, but also provides the basis for an inverse design procedure applicable to high speed configurations.

INTRODUCTION

Impact theory and linear theory have provided the basic aerodynamic analysis tools used by the vehicle designer in the supersonic and hypersonic speed ranges. The linear theory methods, e.g., References 1 to 3, apply in the supersonic range, while impact theory methods, Reference 4, are used in the hypersonic range. Strictly speaking, neither method is appropriate in the Mach 4 to 8 range, and both methods may exhibit anomalous, and often severe, failures when applied in that speed range. The following sections identify the specific nature of these failures, and show how linear theory and impact theory can be combined to provide improved aerodynamic predictions in the Mach 4 to 8 range. Comparisons with experimental pressure data are presented to show that the combined linear theory/impact theory approach gives significantly improved results over either theory applied by itself.

In Reference 5, linear theory was applied in the inverse design mode to investigate the potential gains due to wing camber at high Mach numbers. The results indicated little or no payoff above Mach 5. The present analysis indicates that unmodified linear theory applied in the inverse design mode will underpredict the effectiveness of wing camber in reducing drag-due-to-lift in the Mach 4 to 8 range. In this investigation, the optimization equations are rederived to properly account for the coupling of the thickness and lifting terms, which is excluded from the linear theory analysis. In addition, a procedure for the application of the combined linear theory/impact theory approach in the inverse design mode is illustrated.

In this study, the original Ames version of the Woodward program, Reference 1, and the Hypersonic Arbitrary Body Program or Gentry program, Reference 4, were modified and used for all basic calculations. The Woodward program provides the linear theory influence coefficients, which are used to 'correct' the two-dimensional, non-interference impact pressure distributions calculated using the Gentry program. The modified pressure distributions are then integrated over the Gentry geometry model for aerodynamic forces and moments.

ANALYSIS

Shortcomings of Linear Theory and Impact Theory in Mach 4 to 8 Range

Linear Theory - Supersonic linear theory is developed from small perturbation considerations. Several of the key assumptions leading to the linearized potential flow equation effectively limit the Mach range and vehicle geometry for which the theory applies. These assumptions are: (1) that the thickness and camber slopes are small, (2) that the products of the perturbation velocities are negligible compared to linear terms in the perturbation quantities, and (3) that the flow is irrotational or isentropic. Assumption (1) places limitations on the vehicle geometry. Supersonically, it means that no slope on the vehicle can be larger than the Mach angle. This restriction makes it very difficult to model real configurations at hypersonic Mach numbers. The second assumption is necessary to linearize the equations, but it also places an upper limit on the Mach range, since the neglected terms are all multiplied by M^2. The third assumption, that the flow is isentropic, implies that shock waves can be approximated by Mach waves. Since the Mach angle is, in general, less than the shock angle, the effect is two-fold. The strength of the wave is incorrectly computed, and the region of influence, i.e., within the Mach cone, is underpredicted. The relative error in the region of influence increases rapidly with Mach number, as shown for a 10° cone in Figure 1. Since the effectiveness of wing camber in reducing drag-due-to-lift depends on the region influenced by each element, this is one of the reasons why unmodified linear theory applied in the inverse design mode shows little or no payoff above Mach 5.

The supersonic linear theory formulations of References 1 to 3, as applied to wings, rely on solutions which uncouple the camber and thickness terms. These solutions neglect the contributions of the thickness slopes to the local lifting pressures. The present study shows that these terms are not negligible above Mach 4, and that they must be included, along with non-linear camber terms, for appropriate aero predictions in the Mach 4 to 8 range.
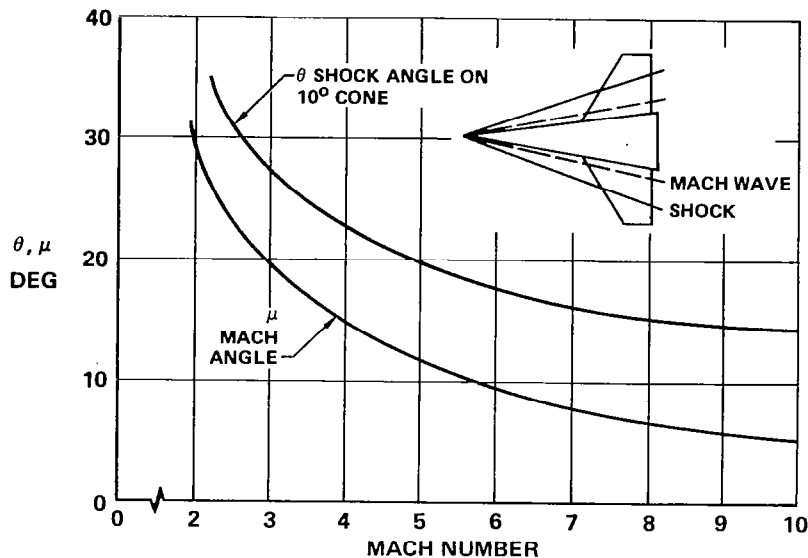
FIGURE 1

COMPARISON OF REGION OF INFLUENCE AS DEFINED BY MACH ANGLE (LINEAR THEORY) AND SHOCK ANGLE ON 10° CONE

The result is that linear theory methods strictly apply below about Mach 3 for configurations that may be characterized as sharp, thin, with small camber, and at low angle of attack.

In addition, various practical problems arise in the translation of the theory into operational computer programs, even in the applicable Mach range. These problems relate to the translation of the geometry of a complex, 3D vehicle into an appropriate linear theory analog for the computer program.

Impact Theory – Newtonian impact theory is based on the assumption that the Mach number is so high ($M \to \infty$) that the shock is nearly coincident with the surface, and that the pressure on the surface is, therefore, only a function of the local surface slope. The implicit assumption is that the Mach angle, and therefore the region of influence from a point, is zero. The result is that impact theory is really two-dimensional. Given a surface element, no account is taken of the effect of adjacent elements, or of the element geometry (sweep, aspect ratio, taper ratio, or tip effects). Thus, the three dimensionality of the vehicle planform and the interference effects are not properly assessed unless the free stream Mach number is very high.

3

Attempts have been made to extend impact theory to lower Mach numbers by introducing a Mach number dependence, as well as surface slope, into the pressure coefficient relation. The result is that there are now some 27 different pressure options to choose from in the Gentry program. While the careful choice of the pressure options applied to complex configurations in the Mach 4 to 8 range generally gives good force and moment predictions, as a rule, the local pressure distributions are not well predicted. For this reason, attempts to optimize high speed configurations using impact theory methods have not been very successful.

Combined Impact Theory/Linear Theory Approach

Impact theory is conceptually and computationally simple, and permits a geometric representation of considerable detail. The method correctly accounts for the nonlinear aerodynamics which characterize the higher Mach range. However, the approach lacks the mechanism for properly assessing both the effect of the local element geometry and the influence of one surface element on another. This mechanism exists in the aerodynamic influence coefficient (AIC) matrix of a number of finite element, linear theory analyses.

The aero influence coefficients, obtained from the solutions to the linearized differential equations governing the supersonic flow field, give the effect of a disturbance on the i-th element and on all other elements of the configuration. Using a chord plane distribution of vortex elements, as in the analysis of Reference 1, the basic linear theory equation can be written

$$[a_{ij}] \{\Delta C_{p_j}\} = \{\alpha_i\} \qquad (1)$$

In the above matrix equation, a_{ij} is the coefficient for the influence of panel i on panel j, ΔC_{p_j} is the pressure difference (vortex strength) across the j-th panel, and α_i is the linearized boundary condition on panel i. In this case, α_i is the sum of the angle of attack, the local camber slope, and the interference onset flow from all other sources, i.e.,

$$\alpha_i = \alpha - \alpha_{c_i} + n_i \qquad (2)$$

Solving equation (1) for the lifting pressures, which requires inverting the AIC matrix,

$$\{\Delta C_{p_j}\} = [a_{ij}^{-1}] \{\alpha_i\}$$

or

$$\Delta C_{p_j} = \sum_i a_{ij}^{-1} \alpha_i \qquad (3)$$

4

Now, the lifting pressure on a 2-D flat plate is given

$$\Delta C_{p_i}^* = \frac{4}{\beta} \alpha_i \qquad (4)$$

where β is $\sqrt{M^2-1}$ and the asterisk denotes the 2-D non-interference pressure. Substituting α_i from equation (4) into (3), we see that the role of the influence coefficients is to correct the 2-D non-interference pressures for three dimensionality and interference effects, i.e.,

$$\Delta C_{p_j} = \frac{\beta}{4} \sum_i a_{ij}^{-1} \Delta C_{p_i}^* \qquad (5)$$

Equation (5) is the basic equation for the combination of linear theory and impact theory. Using appropriate impact pressure options, the Gentry program is used to calculate the 2-D, noninterference pressures over the configuration. The aerodynamic influence coefficients from the Woodward program are then used to modify the upper and lower surface impact pressures using equation (5). The modified pressures are then integrated over the Gentry geometry model for the forces and moments.

The appropriate impact pressure options to be used in this analysis are those which give the correct local compression and expansion pressures on an inclined 2-D flat plate. These are the oblique shock (or tangent wedge) relation for compression pressures, and the Prandtl-Meyer relation for expansion pressures. For blunted configurations, a pressure option which exhibits Newtonian flow characteristics at deflection angles near 90°, and which fairs smoothly into the oblique shock solution at low angles is needed. The following pressure relation exhibits the desired characteristics,

$$C_p = 2 \frac{\sin\theta \sin\delta}{\cos (\theta-\delta)}$$

where

$$\theta = \mu + \delta - \mu \sin \delta$$

(6)

and δ is the local flow deflection angle and μ is the freestream Mach angle.

VALIDATION OF COMBINED IMPACT THEORY/LINEAR THEORY METHOD

70° Swept Flat Plate at Mach 6.0

The combined Gentry/Woodward analysis was used to calculate the pressures on a 70° swept flat plate at Mach 6 and 8° angle of attack for comparison with unpublished NASA data. The results of the straightforward application of the approach are compared with the data in Figure 2. Also shown in Figure 2 are the

Woodward-alone (pure linear theory) results, and the Gentry-alone (pure impact theory) results. The comparisons show that the spanwise pressure distribution calculated using the combined Gentry/Woodward approach is significantly better than either the basic linear or impact theories.
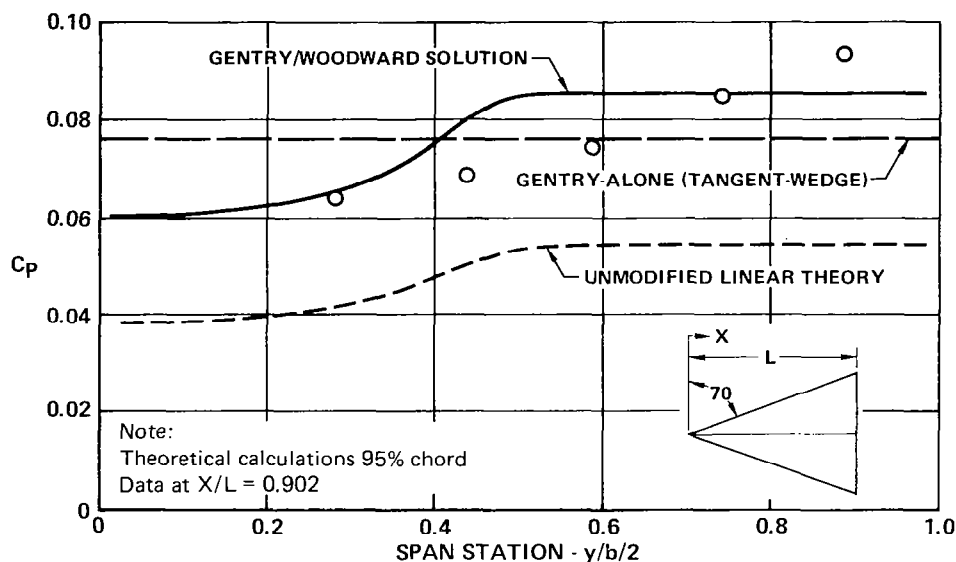
FIGURE 2
PRESSURE COMPARISONS ON 70° SWEPT FLAT PLATE
Mach 6.0 $\alpha = 8°$

Although the straightforward application of the combined approach gives the proper trend and approximately the correct pressure level on the flat plate, the spanwise pressure distribution is shifted too far inboard. This is because the influence coefficients calculated in the Woodward program are based, in part, on the assumption that the region of influence for a given element is contained within a Mach cone corresponding to the freestream Mach number of 6.0. Actually, the average local Mach number, corresponding to the average local pressure on the flat plate, is close to 5.0, and the region of influence based on the average local Mach number is about 20 percent greater than given by the freestream Mach cone. The influence coefficients for this case were recomputed where a spanwise scale factor of 1.2 was used to decrease the span for the linear theory calculation. This spanwise scale factor effectively increases the region of influence to correspond to the average local Mach number on the planform. Figure 3 shows that the use of a spanwise scale factor to correct the region of influence gives improved results. These results support the previous assertion that unmodified linear theory applied at high Mach numbers will tend to underpredict the benefits due to wing camber because the region of influence is underpredicted.

6
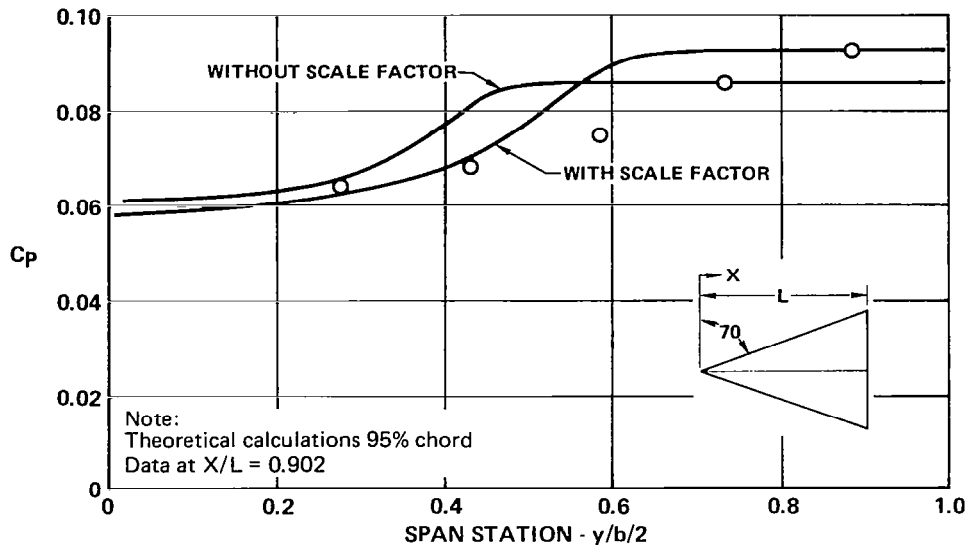
FIGURE 3
EFFECT OF SCALE FACTOR ON GENTRY/WOODWARD SOLUTION
**FOR 70° SWEPT FLAT PLATE**
Mach 6.0 $\alpha = 8°$

76° Swept Wing Comparisons

Experimental pressure data is given in Reference 6 on a 76° swept wing with thickness and camber ($C_{L_{design}}$ = 0.0) for several Mach numbers up to 4.6. The combined Gentry/Woodward program was used to calculate the pressures on this wing at Mach 2.3, 3.5, and 4.6. The results at Mach 4.6 are compared with the data for three angles of attack at six different spanwise stations in Figures 4(a) through 4(f). Also shown are the pressure distributions calculated using both Gentry-alone and Woodward-alone. The Woodward-alone results include the use of a vacuum pressure limit calculation.

At the centerline, Figure 4(a), the pressures calculated with the combined Gentry/Woodward analysis give excellent comparisons with the data, on both the upper and lower surfaces. As might be expected, the comparisons are best for the low angle of attack (5.5°), but even at the highest angle of attack (20.5°), which is nearly twice the freestream Mach angle, the results are very good. As one moves outboard, Figures 4(b) to 4(f), the combined theory begins to over-predict the pressures at the leading edge, and this over-prediction grows progressively worse toward the tip. At the same time, the Gentry-alone pressures compare better and better with the data as one moves outboard.

7
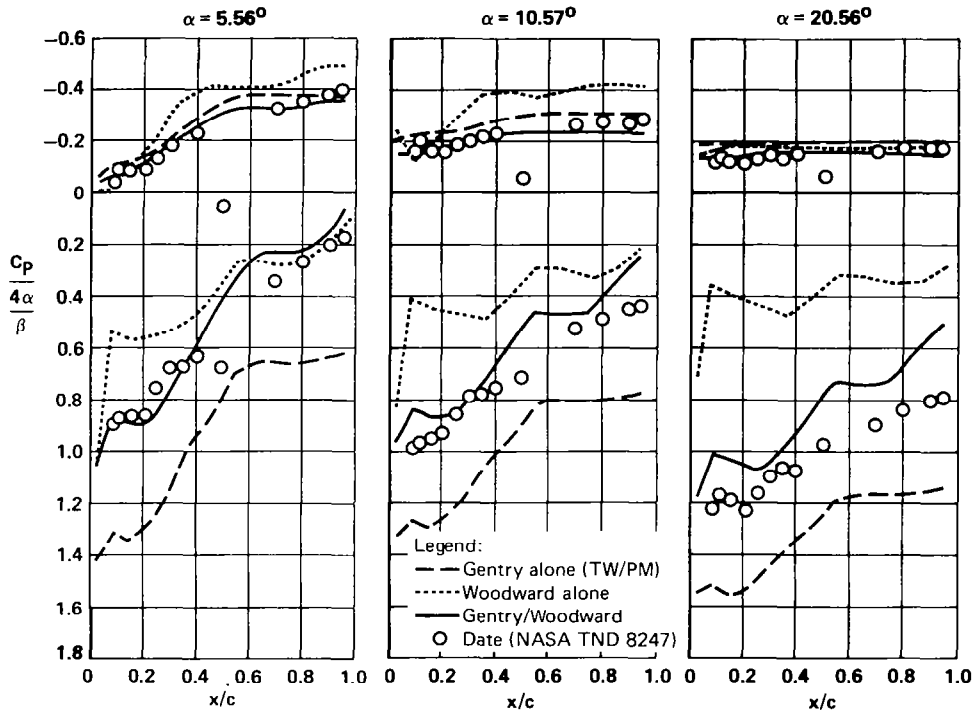
FIGURE 4 (a)
PRESSURE DISTRIBUTIONS ON 76° SWEPT WING
Mach 4.6   Span Station (y/b/2) = 0.0
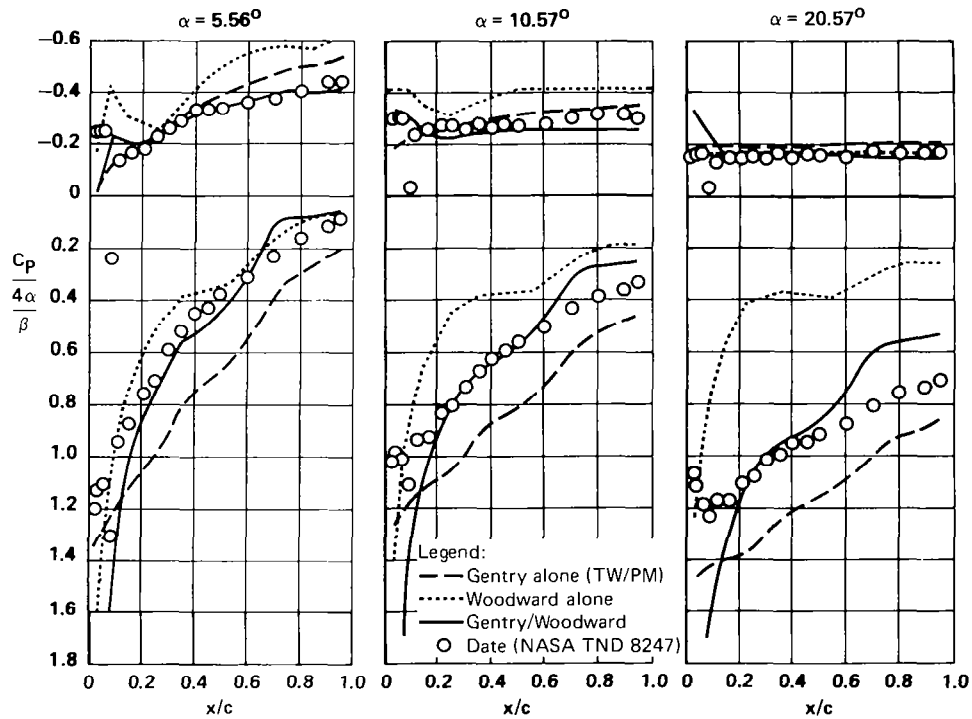
FIGURE 4 (b)
PRESSURE DISTRIBUTION ON 76° SWEPT WING
Mach 4.6   Span Station (y/b/2) = 0.2
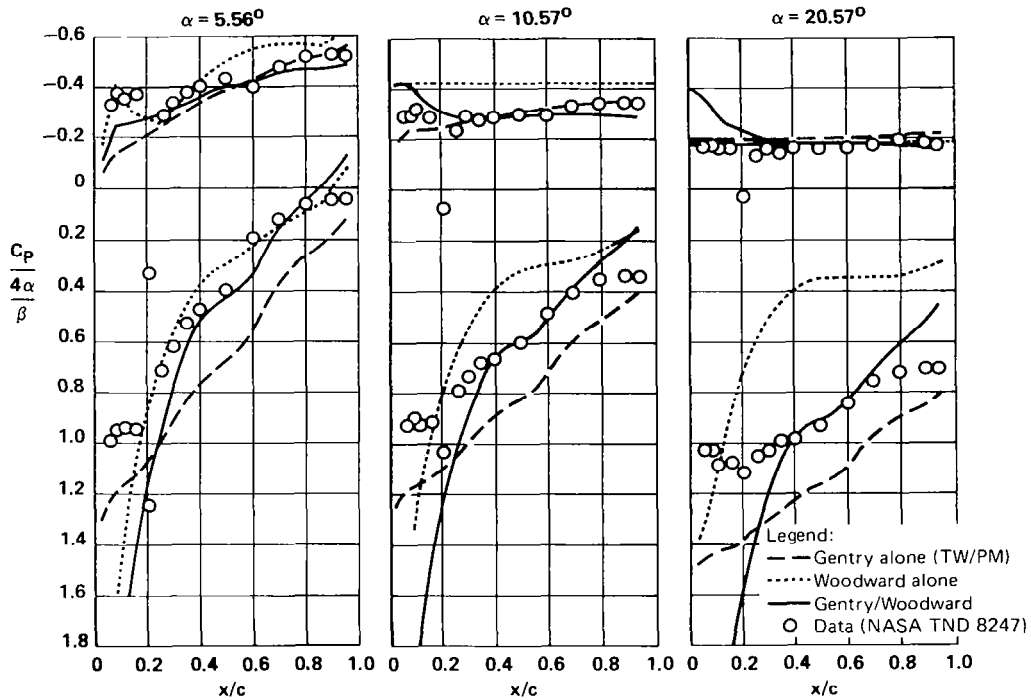
FIGURE 4 (c)
PRESSURE DISTRIBUTION ON 76° SWEPT WING
Mach 4.6   Span Station (y/b/2) = 0.4

FIGURE 4 (d)
PRESSURE DISTRIBUTION ON 76° SWEPT WING
Mach 4.6   Span Station (y/b/2) = 0.6

FIGURE 4 (e)
PRESSURE DISTRIBUTION ON 76° SWEPT WING
Mach 4.6   Span Station (y/b/2) = 0.8
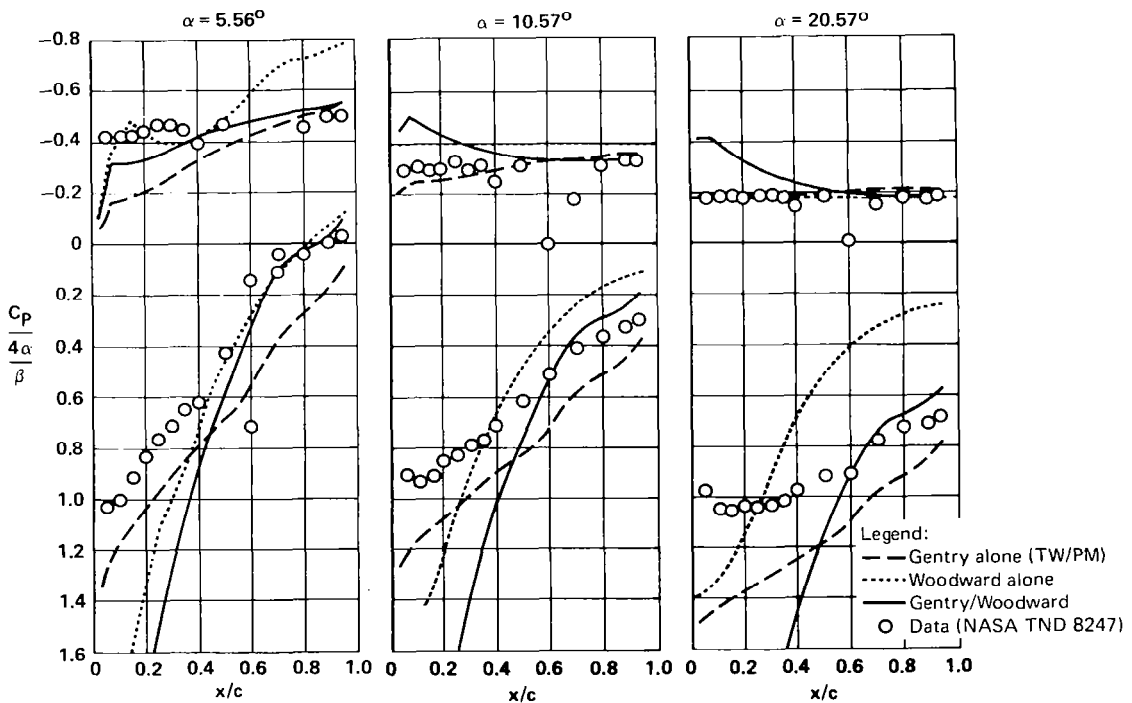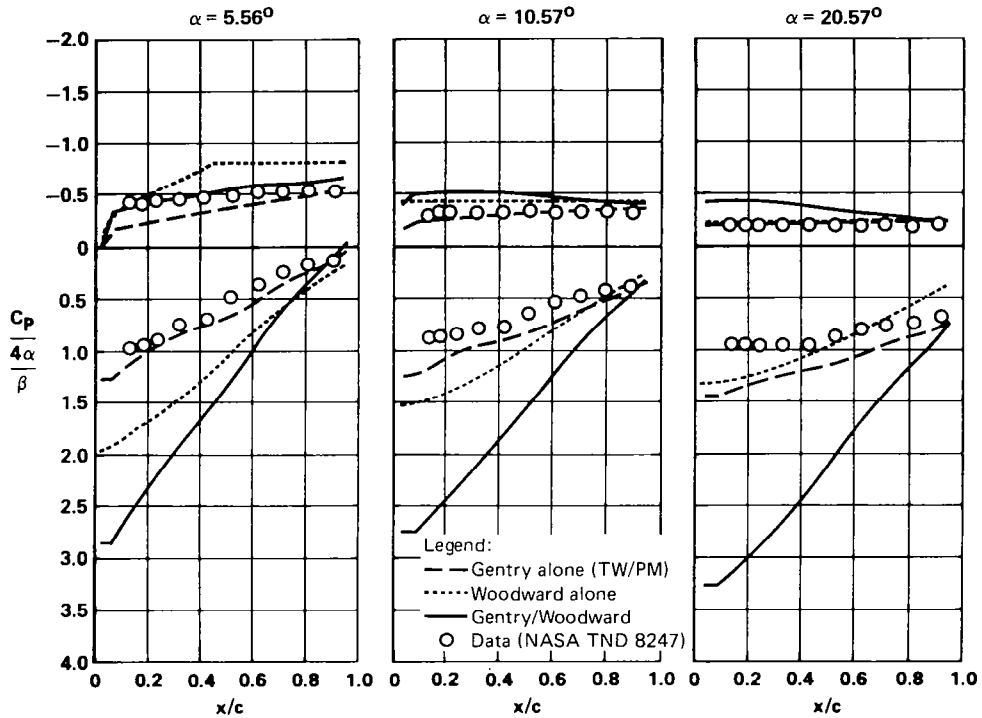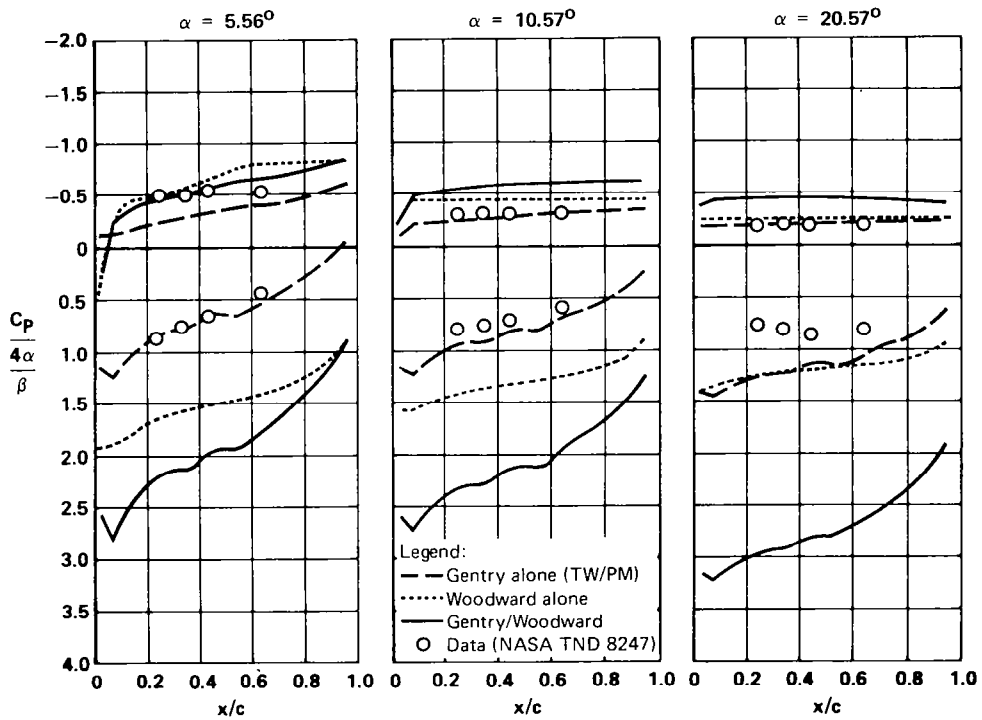

FIGURE 4 (f)
PRESSURE DISTRIBUTION ON 76° SWEPT WING
Mach 4.6   Span Station (y/b/2) = 0.95

10

The over-predictions in the region of the leading edge result from the linear theory influence coefficients. Comparisons with the closed form linear theory solutions for triangular flat plates, given in Reference 7, show that the influence coefficients from the Woodward program are correctly calculated. The indication is that the linear theory solution is inappropriate in the region of the leading edge when the planform has thickness and the leading edge is swept near or aft of the Mach cone. It is believed that this problem arises from the linearization of the basic supersonic flow equation. This problem can be expected to persist until an improved method of calculating the influence coefficients becomes available.

Inspection of the Gentry/Woodward and Gentry-alone comparisons in Figure 4 gives rise to the following empirical rule for correcting the leading edge over-predictions: In the region where the Gentry/Woodward compression pressure is greater than the Gentry-alone pressure, use the Gentry solution, otherwise use the Gentry/Woodward solution. Comparison with the data shows that application of this rule gives reasonably good results at all wing stations. Figure 5 shows that, even though the local pressures are not uniformly well predicted at all points, the method gives excellent predictions of the pressure differences at all wing stations. In addition, this simple rule has the advantages of being locally determined and easily programmed.
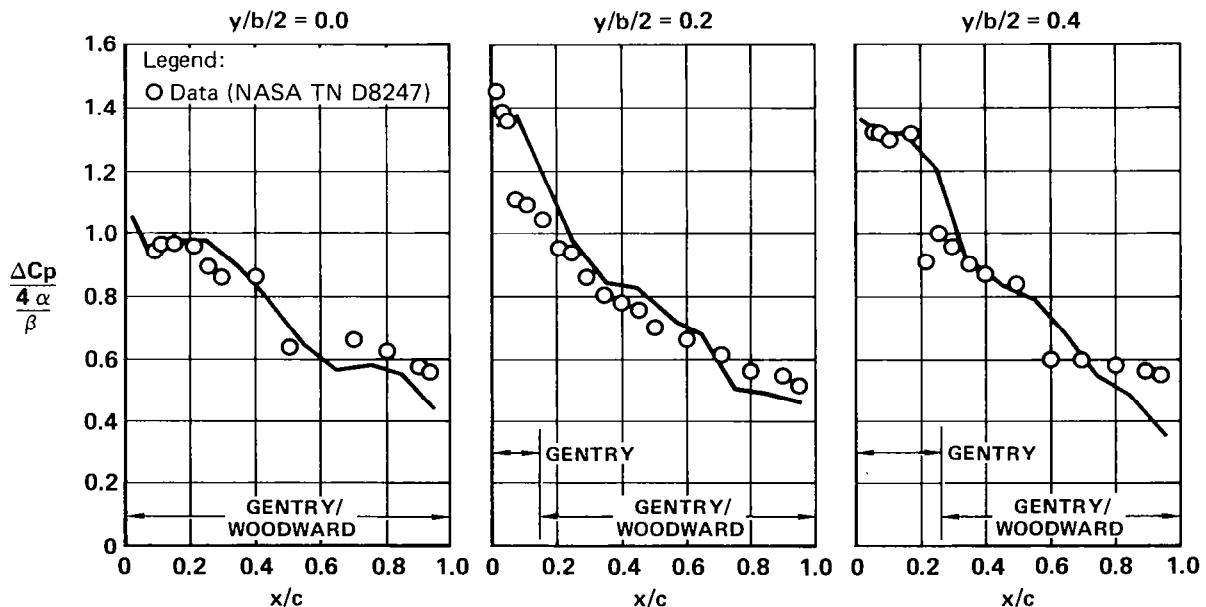
FIGURE 5 (a)
PRESSURE DIFFERENCES ON 76° SWEPT WING USING CURRENT METHOD
Mach 4.6 $\alpha = 5.56°$
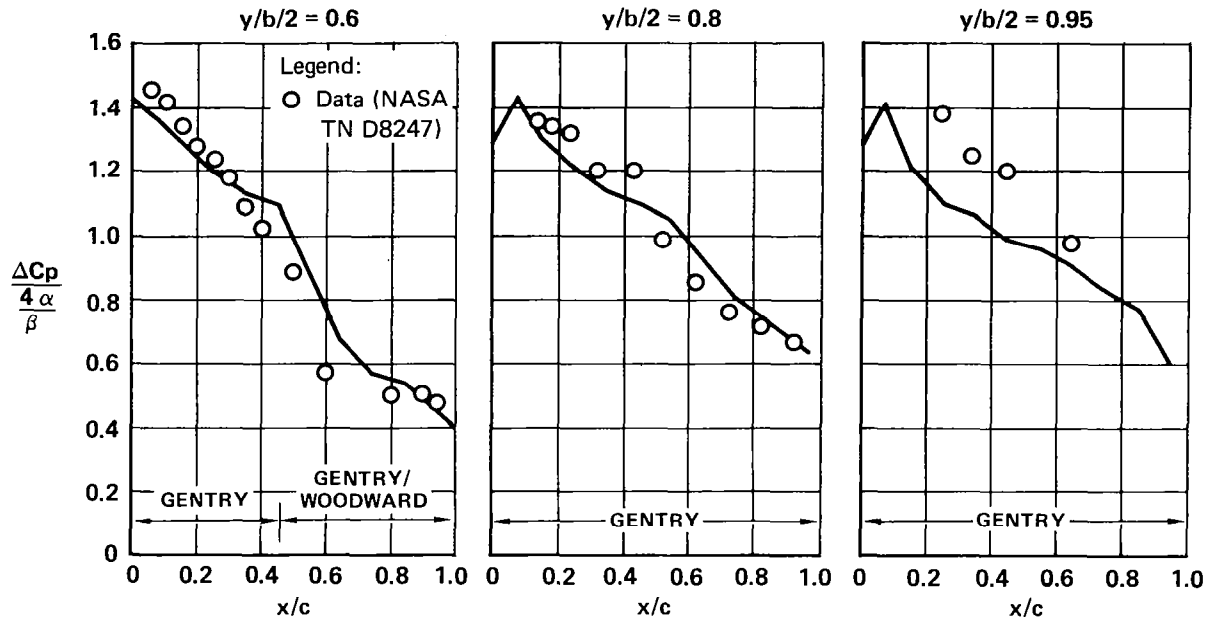
FIGURE 5 (b)
PRESSURE DIFFERENCES ON 76° SWEPT WING USING CURRENT METHOD
Mach 4.6 $\alpha = 5.56°$

Application of the above rule also provides a method for correcting the uninverted aero influence coefficient matrix elements, which are used in the inverse design method. Using equation (5), the Gentry/Woodward pressure on the j-th element is computed from

$$C_{p_j} = \sum_i a_{ij}^{-1} \frac{\beta}{4} C_{p_i}^*$$ (7)

where $C_{p_i}^*$ is the impact pressure on the i-th element, and a_{ij}^{-1} is the influence coefficient which gives the contribution of the i-th element on the j-th panel. If the Gentry/Woodward pressure on the j-th element is greater than the Gentry-alone pressure, i.e., $C_{p_j} > C_{p_j}^*$, we assume that we can scale the influence coefficients affecting the j-th panel so that

$$C_{p_j} = C_{p_j}^* = \sum_i (a_{ij}^{-1})_{SCALED} \frac{\beta}{4} C_{p_i}^*$$ (8)

Assuming that the same scale factor is applied to each coefficient affecting the j-th panel, this means that the j-th <u>row</u> in the inverted matrix is multiplied by a constant, and therefore, the j-th <u>column</u> in the original uninverted matrix is divided by that constant. Note that only the influence coefficients affecting the j-th panel are modified.

Additional Comparisons on the 76° Swept Wing

The combined Gentry/Woodward analysis was also used to calculate the pressure distributions on the 76° swept wing at Mach 2.3 and 3.5. The comparisons with the data at Mach 3.5 are given in Figure 6, and the Mach 2.3 results are given in Figure 7. In general, the comparisons are similar to the Mach 4.6 results, but the quality of the local pressure predictions decreases with decreasing Mach number. Since the combined solution at the lower Mach number (2.3) is very close to the pure linear theory solution, as shown in Figure 8, the poorer pressure comparisons are attributed to the linear theory formulation for subsonic leading edges. Nevertheless, the use of the linear theory influence coefficients to correct the impact theory pressures allows the Gentry program to be used to calculate the forces and moments at these low supersonic Mach numbers, as illustrated in Figure 9.
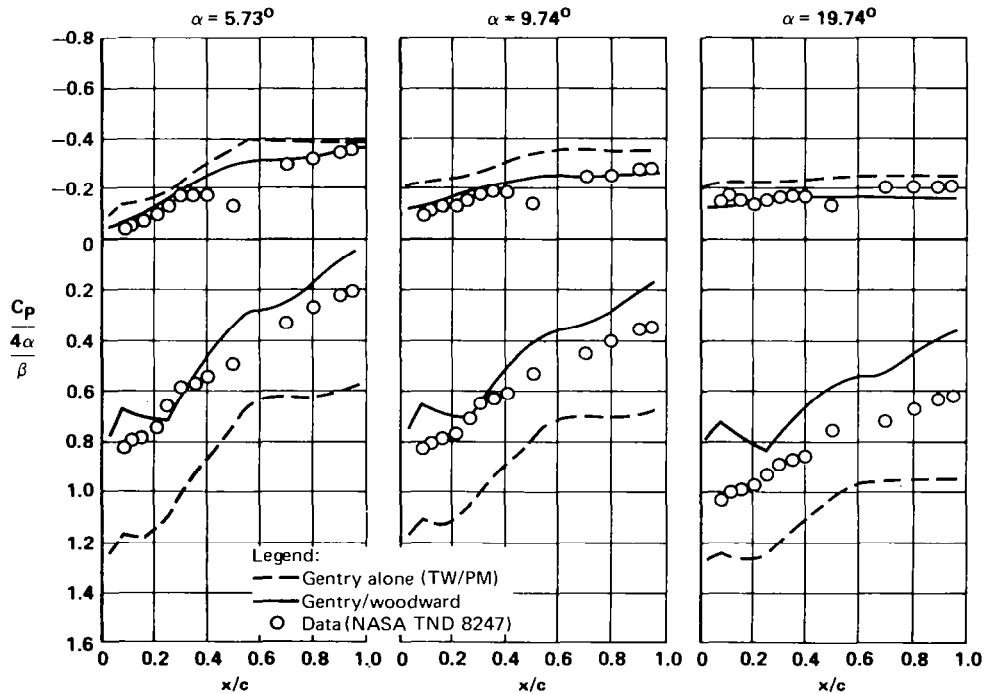
FIGURE 6 (a)
PRESSURE DISTRIBUTION ON 76° SWEPT WING
Mach 3.5   Span Station (y/b/2) = 0.0

FIGURE 6 (b)
PRESSURE DISTRIBUTION 76° SWEPT WING
Mach 3.5   Span Station (y/b/2) = 0.2

FIGURE 6 (c)
PRESSURE DISTRIBUTION ON 76° SWEPT WING
Mach 3.5   Span Station (y/b/2) = 0.4

14
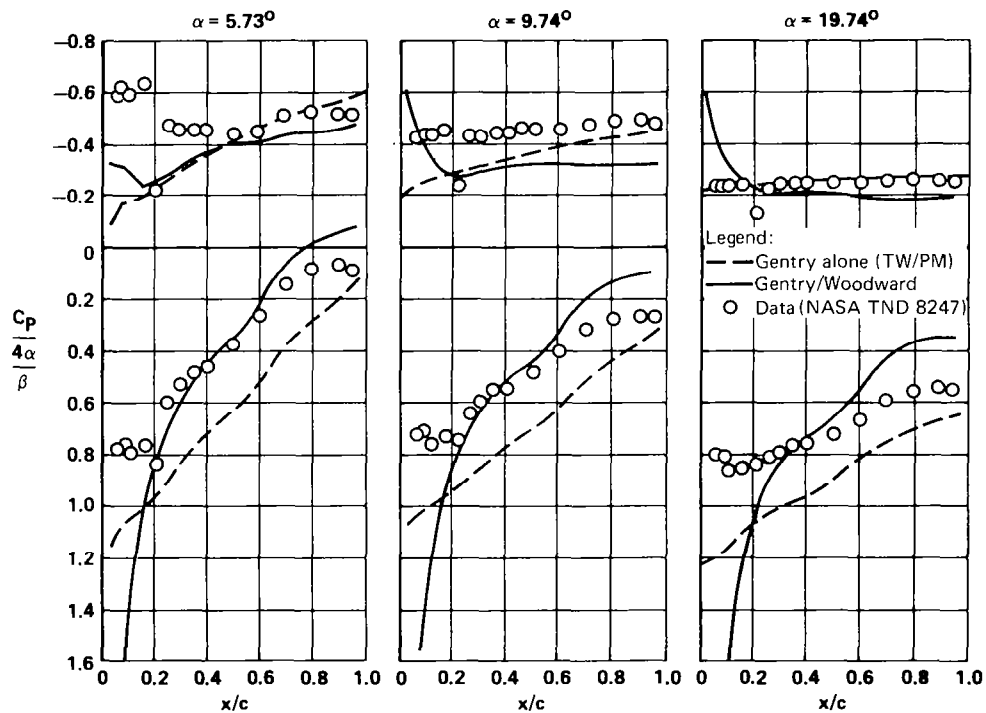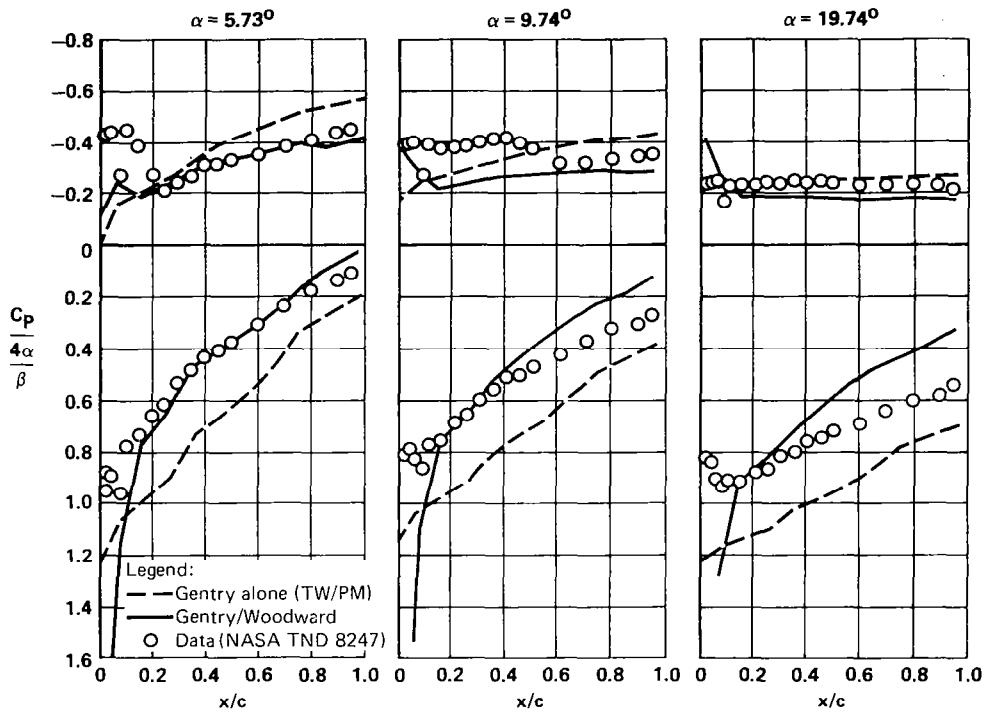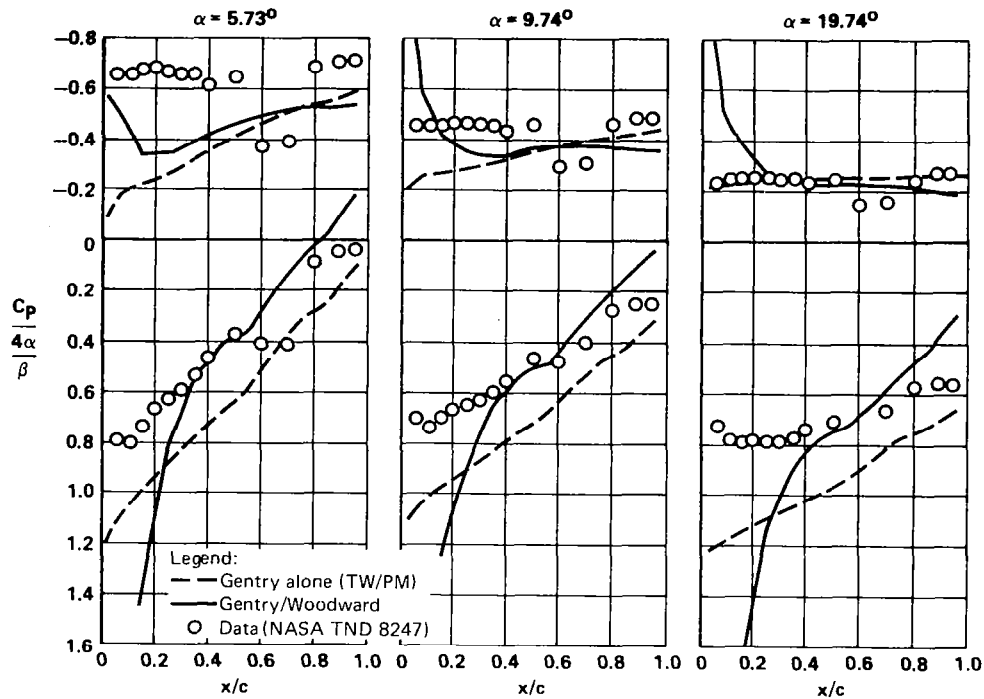
FIGURE 6 (d)
PRESSURE DISTRIBUTION ON 76° SWEPT WING
Mach 3.5   Span Station (y/b/2) = 0.6

FIGURE 6 (e)
PRESSURE DISTRIBUTION ON 76° SWEPT WING
Mach 3.5   Span Station (y/b/2) = 0.8

15
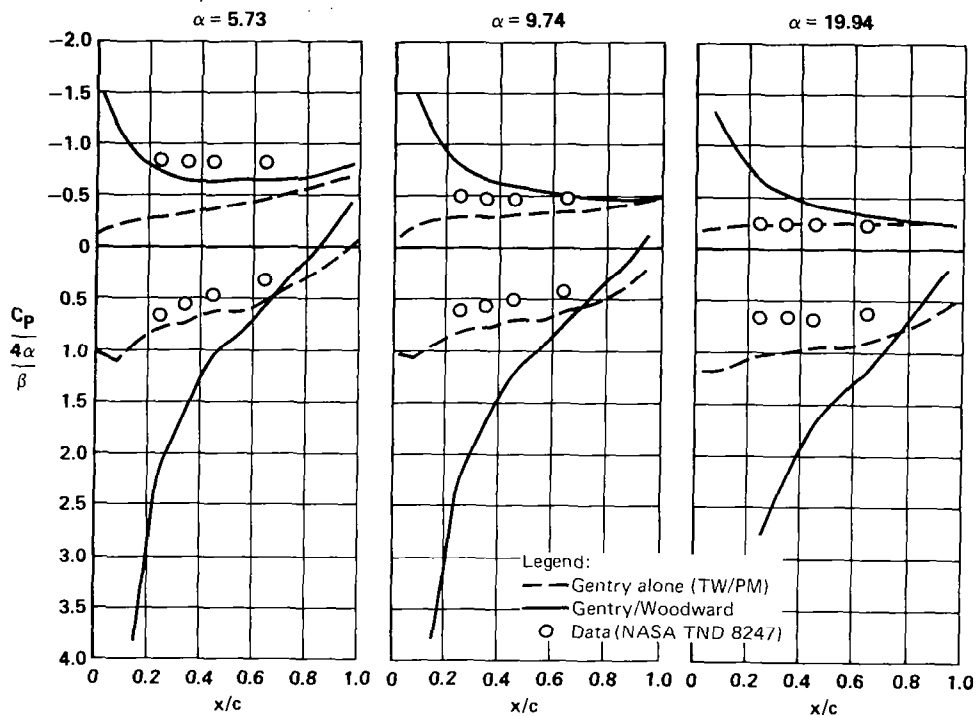
FIGURE 6 (f)
PRESSURE DISTRIBUTION ON 76° SWEPT WING
Mach 3.5   Span Station (y/b/2) = 0.95
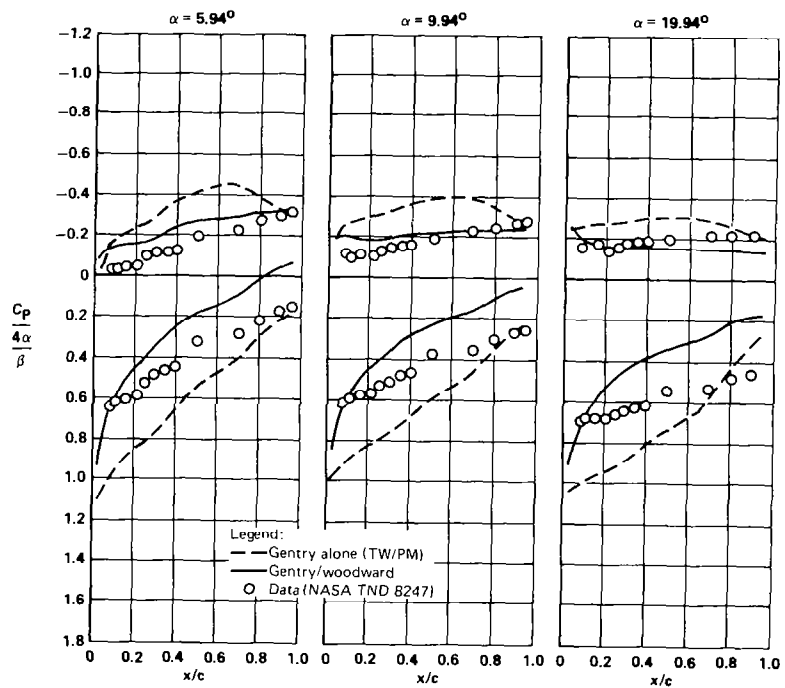
FIGURE 7 (a)
PRESSURE DISTRIBUTIONS ON 76° SWEPT WING
Mach 2.3   Span Station (y/b/2) = 0

16
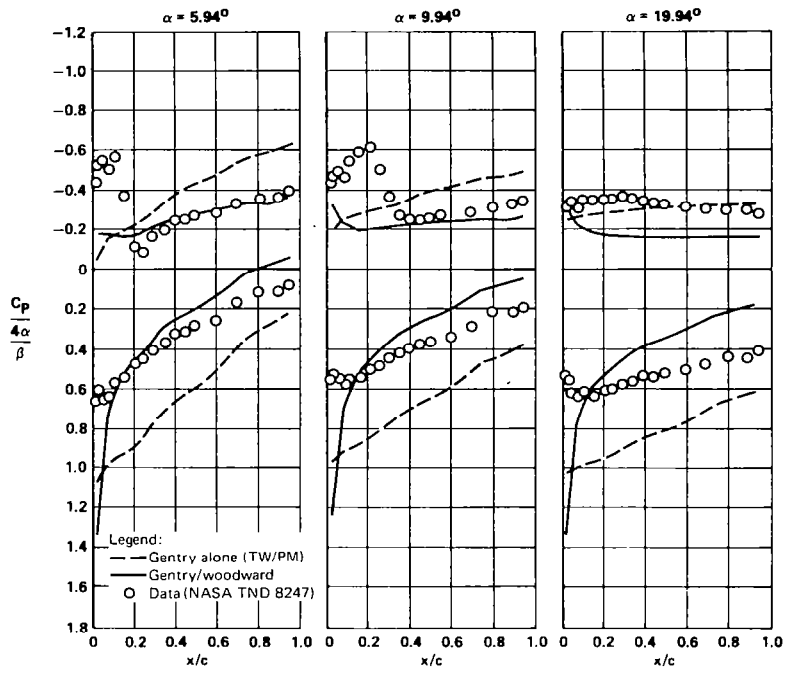
FIGURE 7 (b)

PRESSURE DISTRIBUTIONS ON 76° SWEPT WING

Mach 2.3   Span Station (y/b/2) = 0.2
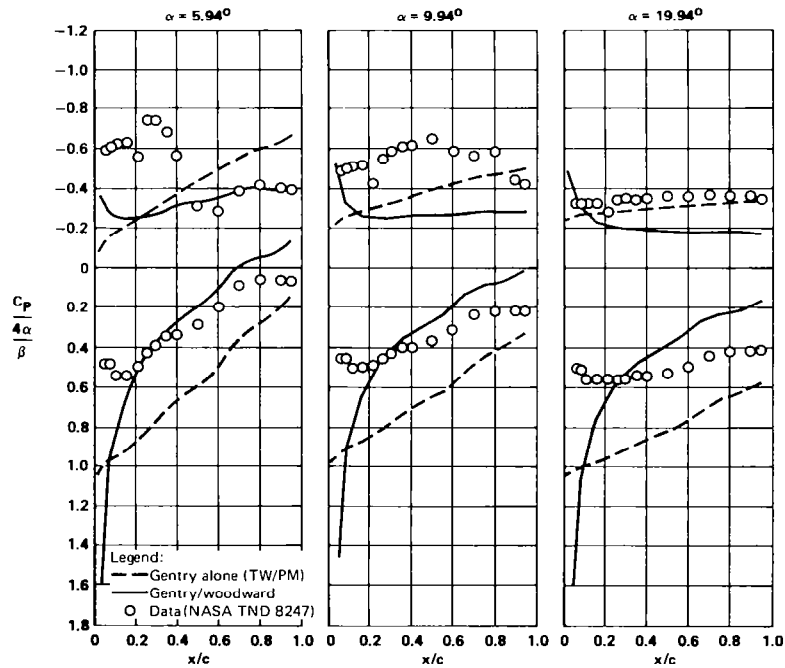
FIGURE 7 (c)

PRESSURE DISTRIBUTION ON 76° SWEPT WING

Mach 2.3   Span Station (y/b/2) = 0.4
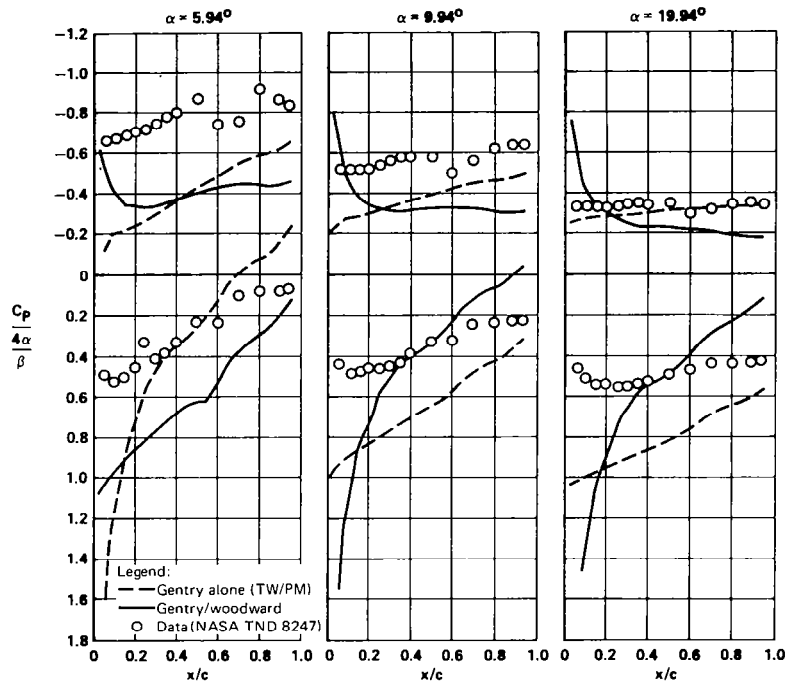
FIGURE 7 (d)
PRESSURE DISTRIBUTION ON 76° SWEPT WING
Mach 2.3   Span Station (y/b/2) = 0.6
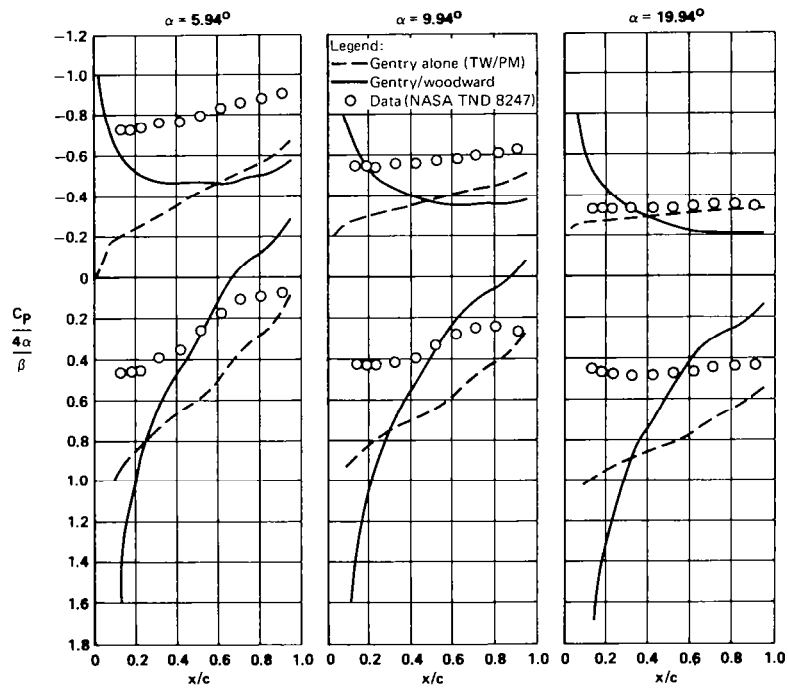
FIGURE 7 (e)
PRESSURE DISTRIBUTION ON 76° SWEPT WING
Mach 2.3   Span Station (y/b/2) = 0.8
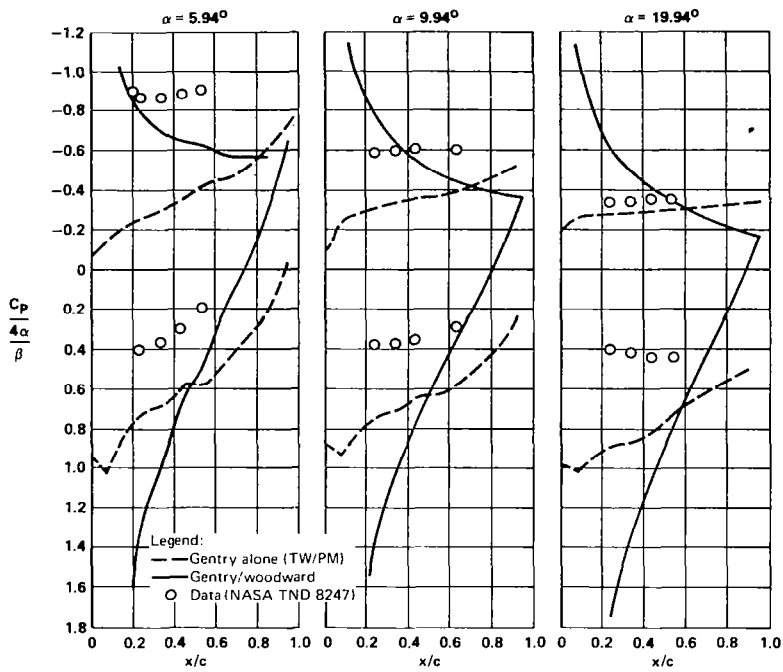
FIGURE 7 (f)
PRESSURE DISTRIBUTION ON 76° SWEPT WING
Mach 2.3   Span Station (y/b/2) = 0.95
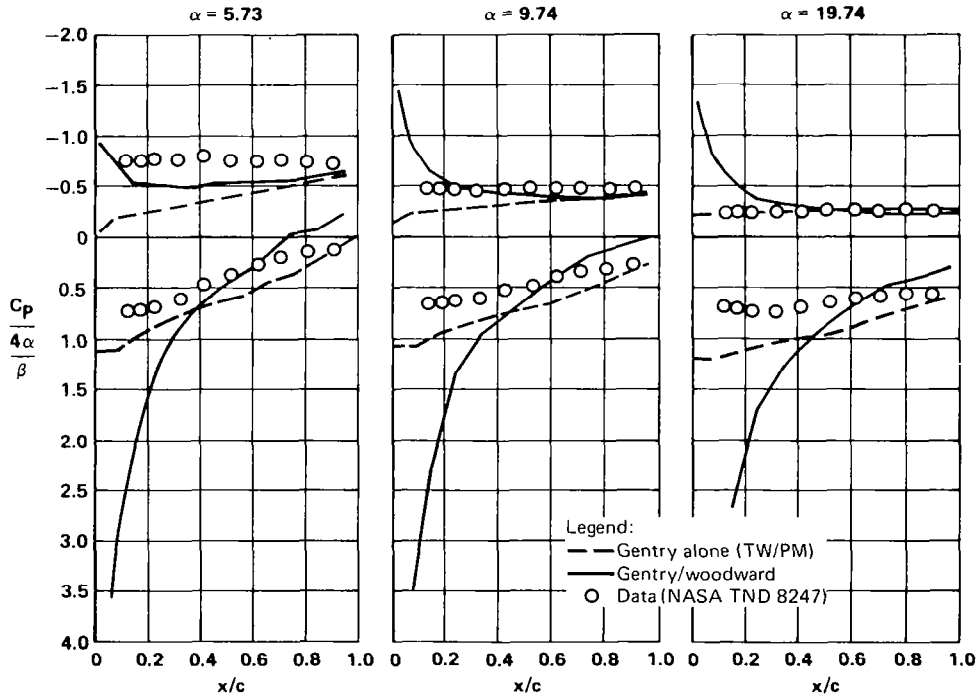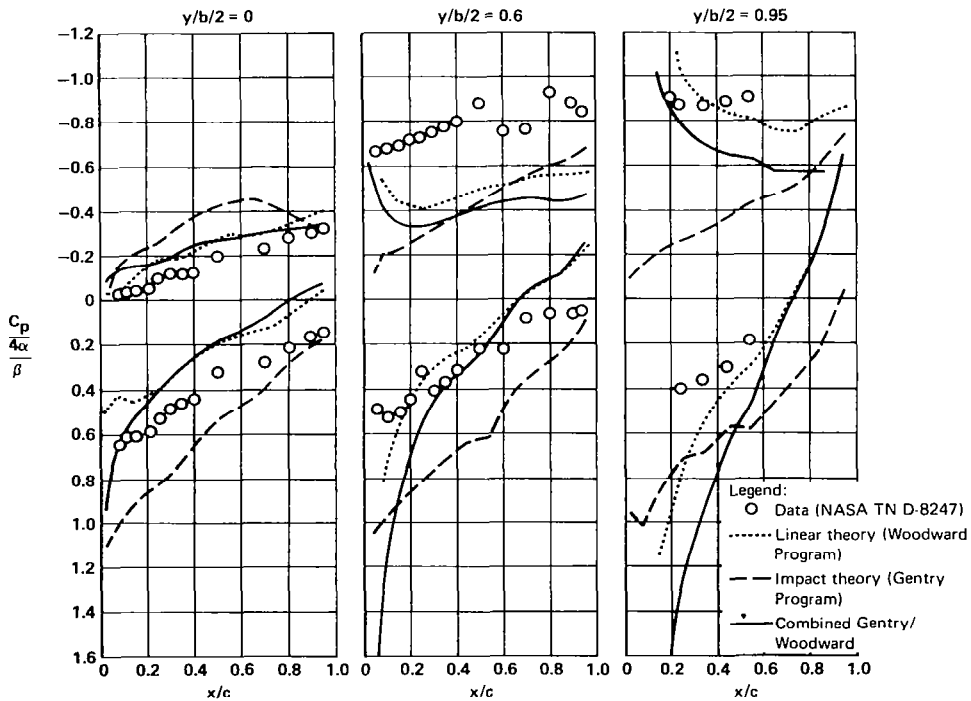

FIGURE 8
COMPARISON OF LINEAR THEORY, IMPACT THEORY AND COMBINED APPROACH
FOR PRESSURES ON 76° SWEPT WING
Mach 2.3 α = 5.94

19
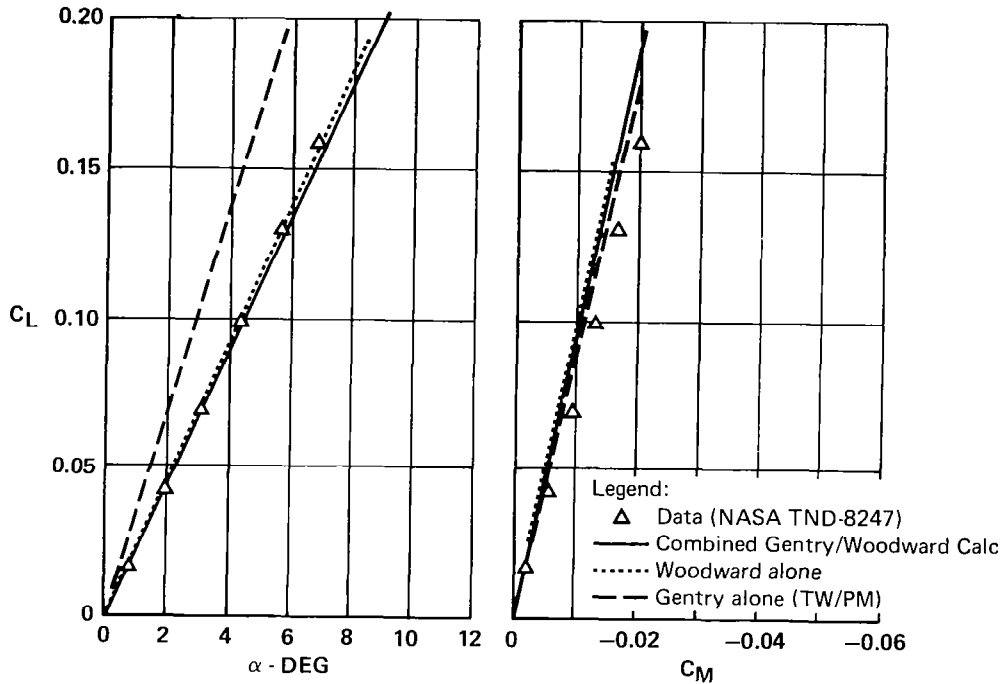
FIGURE 9
LIFT AND MOMENT ON 76° SWEPT WING AT MACH 2.3

Legend:
△ Data (NASA TND-8247)
⎯ Combined Gentry/Woodward Calc
······· Woodward alone
— — Gentry alone (TW/PM)

Ames All-Body Models

The combined impact theory/linear analysis was applied to the NASA Ames All-Body models illustrated in Figure 10. The Gentry/Woodward program was used to calculate the lift and moment on the elliptical cone model (B5) at Mach numbers 2.0 and 5.37. The predictions are compared with the data from Reference 8 in Figures 11 and 12 and show that the combined analysis can be applied across the Mach range to obtain results equal to, or better than, either linear theory or impact theory used alone. The lift comparisons at both Mach numbers indicate that there is a thickness contribution to the lift which is not predicted by linear theory. The importance of these thickness contributions, particularly as they relate to an inverse design method in the Mach 4 to 8 range, are discussed below.

BODY B$_1$ - ELLIPTICAL FOREBODY/CLOSED AFTERBODY

ℓ = 0.4826 m
s   = 0.06241 m^2
x_{REF} = 0.2654 m
c   = 0.3219 m
2b   = 0.2586 m
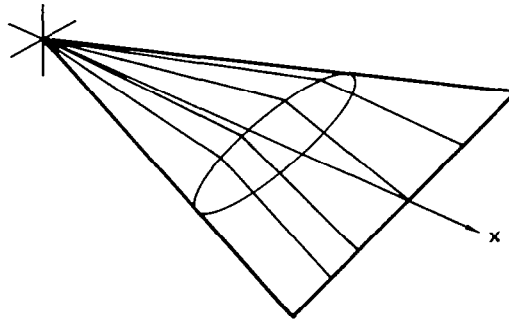
BODY B$_5$ - ELLIPTICAL CONE (SAME AS B$_1$ FOREBODY)
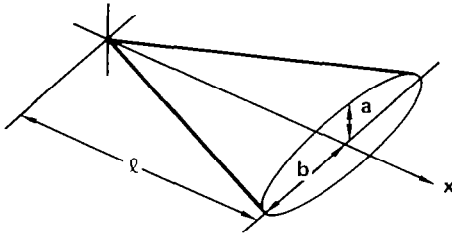
ℓ = 0.322 m
s   = 0.0277 m^2
A_{BASE}= 0.00584 m^2
a   = 0.0216 m
b   = 0.0862 m
x_{REF} = 0.177 m
c   = 0.215 m

FIGURE 10
NASA AMES ALL-BODY MODELS B$_1$ AND B$_5$

Legend:
△ Data (NASA TND-6821)
——— Combined Gentry/Woodward Calc
— — Gentry alone (TW/PM)
· · · · · Linear theory
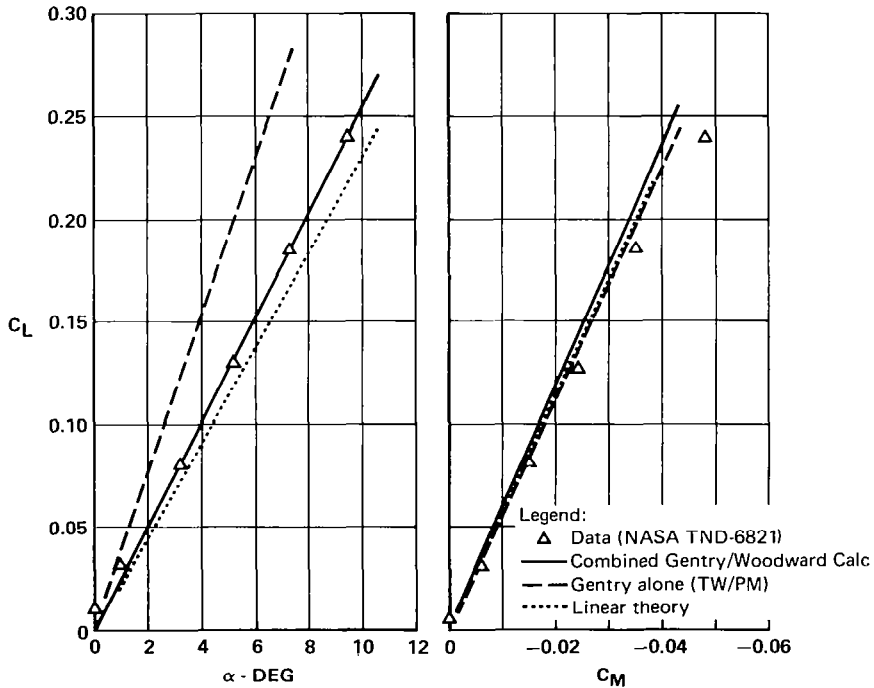
FIGURE 11
LIFT AND MOMENT PREDICTIONS ON AMES ALL-BODY MODEL B$_5$
Mach 2.0

21
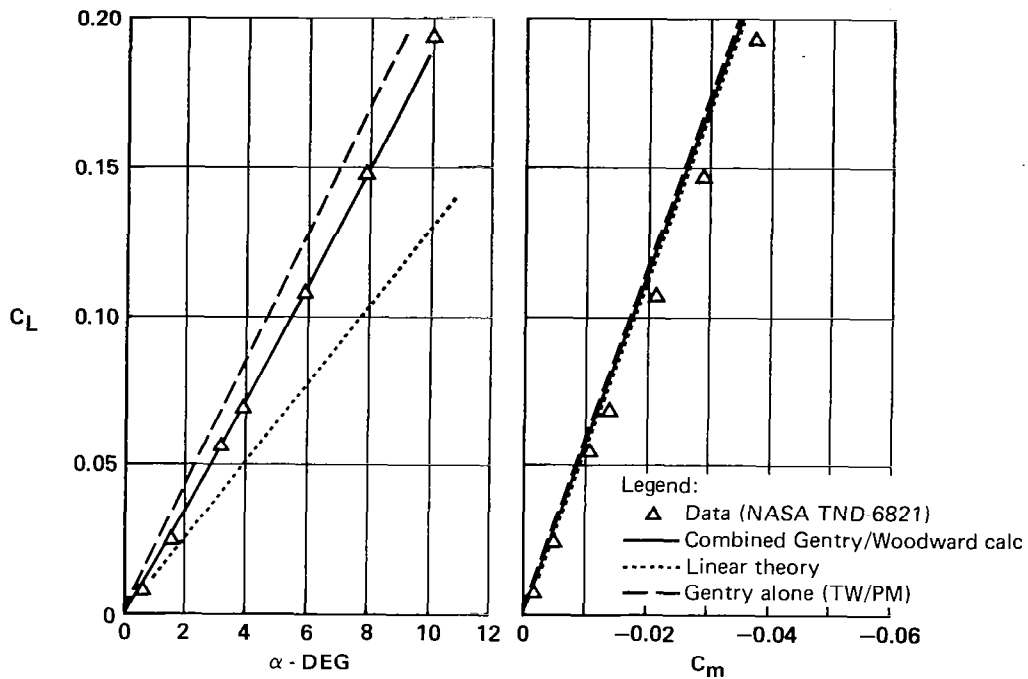
FIGURE 12
LIFT AND MOMENT PREDICTIONS ON AMES ALL-BODY MODEL B$_5$
Mach 5.37

Closed Form Solutions for Lift, Drag, and Moment

Starting with the basic relation for combining linear theory and impact theory, the impact pressure differences obtained from the small angle expansions of the oblique shock and Prandtl-Meyer relations were substituted into Equation (5). The equation was then expanded further to give the lifting pressure in terms of the influence coefficients, the slope of the camber line measured from the freestream, and the local thickness slope. The resulting expression for the lifting pressure was then summed over the planform for the lift, moment, and drag-due-to-lift. With the exception of higher order terms in local camber slope, the resulting summations could be identified as the linear theory contributions to the lift, drag, and moment, or in the case of the thickness terms, using fairly general approximations, could be replaced by integrable expressions. From these expansions, then, closed form expressions were derived for the lift, drag, and moment for uncambered bodies. These closed form expressions, given in Figure 13, require only the lift and moment curve slopes as calculated from linear theory, the angle of attack, and the base area and volume of the configuration.

22

LIFT COEFFICIENT

$$\widetilde{C}_L = (C_{L_\alpha})_{L.T.} \, \alpha \left(1 + \frac{\beta^{3/2}}{5.2} \alpha^2\right) + 2.4\,\alpha\,(C_{L_\alpha})_{L.T.} \left(\frac{\beta}{4}\right) f \frac{A_{BASE}}{S}$$

MOMENT COEFFICIENT

$$\widetilde{C}_M = (C_{M_\alpha})_{L.T.} \, \alpha \left(1 + \frac{\beta^{3/2}}{5.2} \alpha^2\right) + 2.4\,\alpha\,(C_{L_\alpha})_{L.T.} \left(\frac{\beta}{4}\right) f \left\{ \frac{x_{REF} - x_{TE}}{\bar{c}} \frac{A_{BASE}}{S} + \frac{V}{\bar{c}S} \right\}$$

DRAG COEFFICIENT

$$(\widetilde{C}_D - C_{D_{THICK}}) = \widetilde{C}_L \, \alpha + 1.2\,(C_{L_\alpha})_{L.T.} \left(\frac{\beta}{4}\right) f \alpha^2 \frac{A_{BASE}}{S}$$

WHERE:

α	=	ANGLE OF ATTACK
$(C_{L_\alpha})_{L.T.}$	=	LINEAR THEORY (FLAT PLATE) LIFT CURVE SLOPE
β	=	$\sqrt{M^2 - 1}$
f	=	PLAN AREA/(1/2 WETTED AREA)
S	=	PLAN AREA
A_{BASE}	=	BASE AREA
V	=	VOLUME OF CONFIGURATION

FIGURE 13

CLOSED FORM EXPRESSIONS FOR LIFT, MOMENT AND DRAG-DUE-TO-LIFT FOR UNCAMBERED CONFIGURATIONS

The closed form expressions were used to calculate the characteristics at Mach 5.37 and 7.38 on the Ames All-Body models illustrated in Figure 10. The results are compared with the data in Figures 14 and 15. These results show that if the configuration has a base area, then there is a thickness contribution to lift curve slope which is proportional to the base area. Further, even if the configuration is closed at the base (zero base area), there is a thickness contribution to the moment curve slope (C_{M_α}) which is proportional to the volume. These results demonstrate that, in general, the thickness terms must be included in the inverse design procedure to ensure that the optimum camber distributions correspond to the actual lift and moment constraints.

Body	Data	Closed Form Calculations	$\dfrac{S}{S_{ref}}$	$\dfrac{A_{base}}{S_{ref}}$	$\dfrac{Vol}{S_{ref}\,\bar{c}}$	$\dfrac{x_{ref} \cdot x_{CG}}{\bar{c}}$	$\dfrac{x_{ref} \cdot x_{TE}}{\bar{c}}$
B_1	O	——————	1.0	0	0.058	−0.175	−
B_5	Δ	— — —	1.0	0.2104	0.105	−0.175	−0.675

FIGURE 14
CLOSED FORM PREDICTIONS - AMES BODIES B_1 AND B_5
Mach 5.37

Body	Data	Closed Form Calculations	$\dfrac{S}{S_{ref}}$	$\dfrac{A_{base}}{S_{ref}}$	$\dfrac{Vol}{S_{ref}\,\bar{c}}$	$\dfrac{x_{ref} \cdot x_{CG}}{\bar{c}}$	$\dfrac{x_{ref} \cdot x_{TE}}{\bar{c}}$
B_1	O	——————	1.0	0	0.058	−0.175	−
B_5	Δ	— — —	1.0	0.2104	0.105	−0.175	−0.675

FIGURE 15
CLOSED FORM PREDICTIONS - AMES BODIES B_1 AND B_5
Mach 7.38

24

The use of linear theory influence coefficients to correct the impact pressure distributions provides the basis for the use of the method in the inverse design mode. Three things must be taken into account for application in the Mach 4 to 8 range: 1) the influence coefficients in the region of the leading edge must be corrected to prevent the large leading edge overpredictions in the lifting pressures. 2) The thickness contributions to the lifting pressures must be included in the analysis. And, 3) the region of influence must be corrected for large values of $\beta \cot \Lambda$, where Λ is the leading edge sweep.

The method for scaling the influence coefficients in the *region of the leading edge by comparing the linear theory pres-sure to the impact pressures* was previously discussed. Also, the use of a spanwise scale factor to correct the linear theory region of influence was demonstrated for the 70° swept flat plate at Mach 6.0. The remaining task is to show that the thick-ness contributions to the lifting pressures at high Mach numbers can be introduced into the linear theory inverse design procedure.

The small angle expansions of the oblique shock and Prandtl-Meyer relations can be used to give an expression for the impact theory lifting pressure in terms of camber line slope, thickness slope, and Mach number. This expression is

$$\Delta C_{p_i}^* = \frac{4}{\beta} \alpha_i \left(1 + 1.2\beta\varepsilon_i + .6\beta^{3/2} \varepsilon_i^2\right) + .8\beta^{1/2} \alpha_i^3 \qquad (9)$$

where α_i is the slope of the camber line measured from the free-stream, ε_i is the local thickness slope as calculated from the Gentry program for $\alpha_i = 0$, and β is $\sqrt{M^2-1}$. Substituting equa-tion (9) into the basic equation, equation (5), and neglecting the cubic term in α_i, the lifting pressure is

$$\Delta C_{p_j} = \sum_i a_{ij}^{-1} \alpha_i b_i \qquad (10)$$

where b_i is the thickness term in equation (9). With this ex-pression, the optimization equations derived by Woodward in Reference (1) for minimum drag can be rederived, to include the thickness terms. The resulting set of linear equations, for the optimum loadings is given, in matrix form, in Figure 16. Solving this set of equations for the $(\Delta C_{p_j})_{OPTIMUM}$, the corres-ponding optimum camber distributions are calculated from

$$\alpha_i = \frac{1}{b_i} \sum_j a_{ij} (\Delta C_{p_j})_{OPT} \qquad (11)$$

Note that for zero thickness, $b_i \to 1$, and the optimization equa-tions reduce to the same set derived by Woodward.

OPTIMIZATION MATRIX – Solution gives loadings for minimum drag corresponding to lift and moment constraints

$$
\begin{bmatrix}
(\dfrac{s_1 a_{11}}{b_1} + \dfrac{s_1 a_{11}}{b_1}) & (\dfrac{s_1 a_{12}}{b_1} + \dfrac{s_2 a_{21}}{b_2}) & (\dfrac{s_1 a_{13}}{b_1} + \dfrac{s_3 a_{31}}{b_3}) & \cdots & s_1 & s_1(\bar{x}-x_1) \\[2ex]
(\dfrac{s_2 a_{21}}{b_2} + \dfrac{s_1 a_{12}}{b_1}) & (\dfrac{s_2 a_{22}}{b_2} + \dfrac{s_2 a_{22}}{b_2}) & (\dfrac{s_2 a_{23}}{b_2} + \dfrac{s_3 a_{32}}{b_3}) & \cdots & s_2 & s_2(\bar{x}-x_2) \\[2ex]
(\dfrac{s_3 a_{31}}{b_3} + \dfrac{s_1 a_{13}}{b_1}) & (\dfrac{s_3 a_{32}}{b_3} + \dfrac{s_2 a_{23}}{b_2}) & (\dfrac{s_3 a_{33}}{b_3} + \dfrac{s_3 a_{33}}{b_3}) & \cdots & s_3 & s_3(\bar{x}-x_3) \\[2ex]
\cdots & & & & & \\[2ex]
s_1 & s_2 & s_3 & \cdots\ 0 & 0 \\[1ex]
s_1(\bar{x}-x_1) & s_2(\bar{x}-x_2) & s_3(\bar{x}-x_3) & \cdots\ 0 & 0
\end{bmatrix}
\begin{bmatrix}
\Delta C_{p_1} \\[2ex] \Delta C_{p_2} \\[2ex] \Delta C_{p_3} \\[2ex] \cdots \\[1ex] \Lambda_1 \\[1ex] \Lambda_2
\end{bmatrix}
=
\begin{bmatrix}
0 \\[2ex] 0 \\[2ex] 0 \\[2ex] \cdots \\[1ex] \bar{L} \\[1ex] \bar{M}
\end{bmatrix}
$$

OPTIMUM CAMBER – calculated from optimum loadings

$$
\alpha_i = \frac{1}{b_i} \sum_j a_{ij} (\Delta C_{p_j})_{OPT}
$$

where

s_i = area of element i

a_{ij} = influence coefficient (element i on element j)

$b_i = 1 + 1.2\beta\epsilon_i + .6\beta^{3/2}\epsilon_i^2$ (thickness factor from Gentry Program)

ΔC_{p_i} = pressure difference on element i

$\bar{x}-x_i$ = distance from moment ref. to centroid of element i

Λ_1, Λ_2 = langrangian multipliers

$\bar{L}, \bar{M}$ = design lift and moment constraints

$$
\bar{L} = \bar{C}_L\, S \qquad \bar{M} = \bar{C}_M\, S\, \bar{c}
$$

FIGURE 16
OPTIMIZATION MATRIX FOR DESIGN PROCEDURE

For large values of camber slope, and/or for very high Mach numbers, the cubic term in camber slope may not be negligible. For this case, an iterative procedure may have to be applied to obtain the actual camber slope. If iteration is necessary, the initial values of the b_i factor would be adjusted using the previously calculated camber slope, so that

$$(b_i)_{iteration} = (b_i)_o + .2\beta^{3/2} (\alpha_i^2)_{previous}$$

where $(b_i)_o$ is the thickness term neglecting the higher order camber term.

The procedure for applying the combined impact theory/linear theory approach is outlined in Figure 17.

GIVEN:
- WING-BODY PLANFORM
- THICKNESS ENVELOPES
- DESIGN LIFT AND MOMENT

INFLUENCE COEFFICIENTS

THICKNESS AND SCALE FACTORS

CAMBER DISTRIBUTION

WOODWARD PROGRAM
- CALCULATE BASIC INFLUENCE COEFFICIENT MATRIX
- CALCULATE INVERTED MATRIX
- CORRECT INFLUENCE COEFFICIENTS
- FORM OPTIMIZATION MATRIX
- CALCULATE OPTIMUM CAMBER SLOPES

GENTRY PROGRAM
- UNCAMBERED SOLUTION AT MODERATE α
- CALCULATE THICKNESS/MACH TERMS
- CALCULATE SCALE FACTORS FOR INFLUENCE COEFFICIENTS
- CALCULATE CHARACTERISTICS ON CAMBERED CONFIGURATION

FIGURE 17
STEPS IN DESIGN PROCEDURE

27

CONCLUDING REMARKS

The results of this study demonstrate that the combination of linear theory and impact theory is a feasible and attractive approach for improved calculations of the aerodynamic characteristics of configurations at high speeds. The application of the combined approach to several wing alone cases shows that the method not only gives improved predictions for local pressures and loadings, but that it also allows the basic Gentry program to be used at low supersonic Mach numbers to predict forces and moments. Additional benefits of the combined approach are 1) it reduces the number of impact pressure coefficient options required to just three basic options, 2) it provides a method for correcting the linear theory influence coefficients to remove the over-predictions in lifting pressures near the leading edge when the planform is swept near the Mach cone, and 3) it provides the basis for an inverse design procedure applicable in the Mach 4 to 8 range.

In the course of the study, the basic relations for the combination of linear theory and impact theory were used to derive closed form expressions for the lift, moment, and drag-due-to-lift of uncambered bodies in terms of the linear theory slopes, the angle of attack, and the base area and volume of the configuration. These expressions should be useful for the preliminary estimation of aerodynamic characteristics, including thickness and non-linear lifting effects, across the Mach range.

Although the procedure has not been applied to wing-body configurations, the results obtained in the present study on several highly swept wings (up to 76°) indicate that extension to wing-bodies is feasible. Two linear theory methods are available for calculating the influence coefficients for the body and body flow field contributions. These are the use of chord plane vortex panels to represent the body, in the manner similar to that described in reference 2, or the use of surface singularities as was done in reference 3.

APPENDIX

CLOSED FORM SOLUTIONS FOR LIFT, DRAG, AND MOMENT
FOR UNCAMBERED CONFIGURATIONS

Basic Equation - The basic equation for the combination of linear theory and impact theory is

$$\Delta C_{p_j} = \sum_i a_{ij}^{-1} \frac{\beta}{4} \Delta C_{p_i}^* \tag{A1}$$

where ΔC_{p_j} is the lifting pressure on element j, a_{ij}^{-1} is the influence coefficient for panel i on element j, $\Delta C_{p_i}^*$ is the 2-D, noninterference lifting pressure on element i, and $\beta = \sqrt{M^2-1}$.

Impact Pressures - The 2-D, noninterference pressures are obtained from small angle expansions of the oblique shock and Prandtl-Meyer relations.

$$C_{p_i}^* \doteq \frac{2}{\beta} \delta_i + 1.2 \delta_i^2 + .4 \sqrt{\beta} \delta_i^3 \tag{A2}$$

in the above expression δ_i is the local surface slope, and

$$(\delta_i)_{LOWER} = \varepsilon_i + \alpha_i$$
$$(\delta_i)_{UPPER} = \varepsilon_i - \alpha_i \tag{A3}$$

where ε_i is the upper surface thickness slope measured from the camber line, and α_i is the slope of the camber line measured from the freestream. If α_{c_i} is the slope of the camber line (dz_c/dx) measured from the reference chord plane, then

$$\alpha_i = \alpha - \alpha_{c_i} \tag{A4}$$

With the above expressions, the 2-D, noninterference lifting pressures, and the thickness pressures are, respectively

$$\Delta C_{p_i}^* = (C_{p_i}^*)_{LOWER} - (C_{p_i}^*)_{UPPER} = \frac{4}{\beta} \alpha_i + 4.8\alpha_i\varepsilon_i + .8\sqrt{\beta}\,(3\varepsilon_i^2 + \alpha_i^2)\alpha_i$$

and

$$\tag{A5}$$

$$(C_{p_i}^*)_{LOWER} + (C_{p_i}^*)_{UPPER} = \frac{4}{\beta} \varepsilon_i + 2.4\,(\alpha_i^2 + \varepsilon_i^2) + .8\sqrt{\beta}\,(\varepsilon_i^2 + 3\alpha_i^2)\varepsilon_i$$

Substituting the impact pressure relations (A5) into the basic equation (A1), the combined approaches gives

$$\Delta C_{p_j} = \sum_i a_{ij}^{-1} \alpha_i + .2\beta^{3/2} \sum_i a_{ij}^{-1} \alpha_i^3 + 1.2\beta \sum_i a_{ij}^{-1} \epsilon_i \alpha_i$$

$$+ .6\beta^{3/2} \sum_i a_{ij}^{-1} \epsilon_i^2 \alpha_i$$

and

$$(C_{p_i})_{LOWER} + (C_{p_i})_{UPPER} = \sum_i a_{ij}^{-1} \epsilon_i + .6\beta \sum_i a_{ij}^{-1} \epsilon_i^2$$

$$+ .2\beta^{3/2} \sum_i a_{ij}^{-1} \epsilon_i^3 + .6\beta \sum_i a_{ij}^{-1} \alpha_i^2 + .6\beta^{3/2} \sum_i a_{ij}^{-1} \epsilon_i \alpha_i^2$$

(A6)

<u>Lift, Drag, and Moment</u> - The lift, drag, and moment coefficients are obtained by summing the pressures over the planform areas. Thus

$$C_L S = \sum_j S_j \Delta C_{p_j} - \sum_j S_j [(C_{p_j})_{UPPER} + (C_{p_j})_{LOWER}] \epsilon_j \alpha_j$$

$$C_D S = \sum_j S_j \Delta C_{p_j} \alpha_j + \sum_j S_j [(C_{p_j})_{UPPER} + (C_{p_j})_{LOWER}] \epsilon_j$$

(A7)

$$C_M S \bar{C} = \sum_j S_j \Delta C_{p_j} (\bar{x} - x_j)$$

where S is the planform area, S_j is the area of panel j, $\bar{C}$ is the reference chord, and $(\bar{x} - x_j)$ is the distance from the moment reference center to the centroid of panel j.

Substituting the pressure relations from (A6) into the force and moment relations (A7) we have

$$C_L S = \sum_j S_j \sum_i a_{ij}^{-1} \alpha_i + .2\beta^{3/2} \sum_j S_j \sum_i a_{ij}^{-1} \alpha_i^3$$

$$+ 1.2\beta \sum_j S_j \sum_i a_{ij}^{-1} \alpha_i \epsilon_i + .6\beta^{3/2} \sum_j S_j \sum_i a_{ij}^{-1} \epsilon_i^2 \alpha_i$$

$$- \sum_j S_j \epsilon_j \alpha_j \sum_i a_{ij}^{-1} \epsilon_i + \begin{array}{l} \text{HIGHER} \\ \text{(ORDER)} \\ \text{TERMS} \end{array}$$

$$C_D S = \sum_j S_j \alpha_j \sum_i a_{ij}^{-1} \alpha_i + .2\beta^{3/2} \sum_j S_j \alpha_j \sum_i a_{ij}^{-1} \alpha_i^3$$

$$+ .6\beta^{3/2} \sum_j S_j \epsilon_j \sum_i a_{ij}^{-1} \epsilon_i \alpha_i^2 + 1.2\beta \sum_j S_j \alpha_j \sum_i a_{ij}^{-1} \alpha_i \epsilon_i$$

$$+ .6\beta \sum_j S_j \epsilon_j \sum_i a_{ij}^{-1} \alpha_i^2 + .6\beta^{3/2} \sum_j S_j \alpha_j \sum_i a_{ij}^{-1} \epsilon_i^2 \alpha_i \quad \text{(A8)}$$

$$+ \sum_j S_j \epsilon_j \sum_i a_{ij}^{-1} \epsilon_i + .6\beta \sum_j S_j \epsilon_j \sum_i a_{ij}^{-1} \epsilon_i^2$$

$$+ .2\beta^{3/2} \sum_j S_j \epsilon_j \sum_i a_{ij}^{-1} \epsilon_i^3$$

$$C_M S \overline{C} = \sum_j S_j (\overline{x} - x_j) \sum_i a_{ij}^{-1} \alpha_i + .2\beta^{3/2} \sum_j S_j (\overline{x} - x_j) \sum_i a_{ij}^{-1} \alpha_i^3$$

$$+ 1.2\beta \sum_j S_j (\overline{x} - x_j) \sum_i a_{ij}^{-1} \alpha_i \epsilon_i$$

$$+ .6\beta^{3/2} \sum_j S_j (\overline{x} - x_j) \sum_i a_{ij}^{-1} \alpha_i \epsilon_i^2$$

<u>Identification of Terms</u> - The first summation in each of the above equations is the linear theory contribution for a cambered flat plate. Thus

$$\text{(LIFT)} \quad \sum_j S_j \sum_i a_{ij}^{-1} \alpha_i = (C_L)_{L.T.} S$$

$$\text{(DRAG)} \quad \sum_j S_j \alpha_j \sum_i a_{ij}^{-1} \alpha_i = (C_D)_{L.T.} S \quad \text{(A9)}$$

$$\text{(MOMENT)} \quad \sum_j S_j (\overline{x} - x_j) \sum_i a_{ij}^{-1} \alpha_i = (C_M)_{L.T.} S$$

If the plate is uncambered, then $\alpha_i = \alpha$ and these terms become

(LIFT) $\quad \sum_j S_j \sum_i a_{ij}^{-1} \alpha_i \rightarrow \alpha \sum_j S_j \sum_i a_{ij}^{-1} = \alpha (C_{L_\alpha})_{LT} S$

$$\text{(A10)}$$
$$\text{UNCAMBERED}$$

(DRAG) $\quad \sum_j S_j \alpha_j \sum_i a_{ij}^{-1} \alpha_i \rightarrow \alpha^2 \sum_j S_j \sum_i a_{ij}^{-1} = \alpha^2 (C_{L_\alpha})_{LT} S$

(MOMENT) $\quad \sum_j S_j (\bar{x} - x_j) \sum_i a_{ij}^{-1} \alpha_i \rightarrow \alpha \sum_j S_j (\bar{x} - x_j) \sum_i a_{ij}^{-1} = \alpha (C_{M_\alpha})_{LT} S \bar{C}$

The second term in each of the expressions in (A8) represent the non-linear contributions of angle of attack and camber slope. For an uncambered configuration, where $\alpha_i = \alpha$, these terms become

(LIFT) $\quad .2\beta^{3/2} \sum_j S_j \sum_i a_{ij}^{-1} \alpha_i^3 \rightarrow .2\beta^{3/2} \alpha^3 \sum_j S_j \sum_i a_{ij}^{-1}$

$$= .2\beta^{3/2} \alpha^3 (C_{L_\alpha})_{LT} S$$

(DRAG) $\quad .2\beta^{3/2} \sum_j S_j \alpha_j \sum_i a_{ij}^{-1} \alpha_i^3 \rightarrow .2\beta^{3/2} \alpha^4 \sum_j S_j \sum_i a_{ij}^{-1}$

$$\text{(A11)}$$
$$\text{UNCAMBERED}$$

$$= .2\beta^{3/2} \alpha^4 (C_{L_\alpha})_{LT} S$$

(MOMENT) $\quad .2\beta^{3/2} \sum_j S_j (\bar{x} - x_j) \sum_i a_{ij}^{-1} \alpha_i^3 \rightarrow$

$$.2\beta^{3/2} \alpha^3 \sum_j S_j (\bar{x} - x_j) \sum_i a_{ij}^{-1}$$

$$= .2\beta^{3/2} \alpha^3 (C_{M_\alpha})_{LT} S \bar{C}$$

In the drag expression (A8), the last three terms give the drag due to thickness (or wave drag). We will simply replace these terms by $C_{D_{THICK}} S$.

Uncambered Expressions ($\alpha_i = \alpha$) - Using the above expressions, the equations (A8) are rewritten

$$C_L \, S = (C_{L_\alpha})_{LT} \, S \, \alpha (1 + .2\beta^{3/2} \, \alpha^2) + 1.2\beta \, \alpha \sum_j S_j \sum_i a_{ij}^{-1} \, \epsilon_i$$

$$+ .6\beta^{3/2} \, \alpha \sum_j S_j \sum_i a_{ij}^{-1} \, \epsilon_i^2 - \alpha \sum_j S_j \, \epsilon_j \sum_i a_{ij}^{-1} \, \epsilon_i$$

$$(C_D - C_{D_{THICK}}) S = (C_{L_\alpha})_{LT} \, S \, \alpha^2 (1 + .2\beta^{3/2} \, \alpha^2)$$

$$+ 1.2\beta \, \alpha^2 \sum_j S_j \sum_i a_{ij}^{-1} \, \epsilon_i + .6\beta^{3/2} \, \alpha^2 [\sum_j S_j \sum_i a_{ij}^{-1} \, \epsilon_i^2$$

$$\qquad\qquad\qquad\qquad\qquad\qquad\qquad\qquad\qquad\qquad (A12)$$

$$+ \sum_j S_j \, \epsilon_j \sum_i a_{ij}^{-1} \, \epsilon_i] + .6\beta \, \alpha^2 \sum_j S_j \, \epsilon_j \sum_i a_{ij}^{-1}$$

$$C_M \, S \, \bar{C} = (C_{M_\alpha})_{LT} \, S \, \bar{C} \, \alpha (1 + .2\beta^{3/2} \, \alpha^2)$$

$$+ 1.2\beta \, \alpha \sum_j S_j \, (\bar{x} - x_j) \sum_i a_{ij}^{-1} \, \epsilon_i$$

$$+ .6\beta^{3/2} \, \alpha \sum_j S_j \, (\bar{x} - x_j) \sum_j a_{ij}^{-1} \, \epsilon_i^2$$

Thickness Terms - The summations in equation (A12) which are linear in thickness slope can be evaluated under certain conditions. For instance, if the thickness slope is constant over the configuration:

$$\sum_j S_j \sum_i a_{ij}^{-1} \, \epsilon_i = \epsilon_o \sum_j S_j \sum_i a_{ij}^{-1} = \epsilon_o S \, (C_{L_\alpha})_{L.T.} = \frac{A_{BASE}}{2} (C_{L_\alpha})_{LT}$$

At very high Mach numbers ($M \to \infty$), there is no influence of one element on another. For this case, the influence coefficients are

$$a_{ij}^{-1} = 0 \text{ for } i \neq j, \text{ and } a_{ij}^{-1} = \frac{4}{\beta} \text{ for } i = j$$

Then
$$\sum_i a_{ij}^{-1} \, \epsilon_i = \frac{4}{\beta} \, \epsilon_j$$

and

$$\sum_j S_j \sum_i a_{ij}^{-1} \, \epsilon_i = \frac{4}{\beta} \sum_j S_j \, \epsilon_j \to \frac{4}{\beta} \int_{-b/2}^{b/2} \int_0^{Z_{TE}} (\frac{dz}{dx}) \, dx \, dy$$

$$= \frac{4}{\beta} \, \frac{A_{BASE}}{2} = (C_{L_\alpha})_{LT} \, \frac{A_{BASE}}{2}$$

where the linear theory lift curve slope approaches $4/\beta$ at hypersonic Mach numbers.

The same result is obtained for an unswept wing at all supersonic Mach numbers.

From the above considerations, we will approximate the influence coefficients in the summations involving thickness by

$$a_{ij}^{-1} = 0 \text{ for } i \neq j, \text{ and } a_{ij}^{-1} = (C_{L_\alpha})_{LT} \text{ for } i = j$$

Then the double summations in equation (A12) can be approximated by single summations.

$$C_L S = (C_{L_\alpha})_{LT} S \alpha (1 + .2\beta^{3/2} \alpha^2) + 1.2\beta \alpha (C_{L_\alpha})_{L.T.} \sum_j S_j \epsilon_j$$

$$+ (.6\beta^{3/2} - 1) \alpha (C_{L_\alpha})_{LT} \sum_j S_j \epsilon_j^2$$

$$(C_D - C_{D_{THICK}}) S = (C_{L_\alpha})_{LT} S \alpha^2 (1 + .2\beta^{3/2} \alpha^2)$$

$$\text{(A13)}$$

$$+ 1.2\beta \alpha^2 (C_{L_\alpha})_{L.T.} \sum_j S_j \epsilon_j + .6\beta \alpha^2 (C_{L_\alpha})_{LT} \sum_j S_j \epsilon_j$$

$$+ 1.2\beta^{3/2} \alpha^2 (C_{L_\alpha})_{LT} \sum_j S_j \epsilon_j^2$$

$$C_M S \bar{C} = (C_{M_\alpha})_{LT} S \bar{C} \alpha (1 + .2\beta^{3/2} \alpha^2) + 1.2\beta \alpha (C_{L_\alpha})_{LT} \sum_j S_j (\bar{x} - x_j) \epsilon_j$$

$$+ .6\beta^{3/2} \alpha (C_{L_\alpha})_{LT} \sum_j S_j (\bar{x} - x_j) \epsilon_j^2$$

Taking the thickness slope to be (dz/dx) and replacing S_j by $dxdy$, we write

$$\sum_j S_j \epsilon_j \rightarrow \int_{-b/2}^{b/2} \int_0^{z_{TE}} \left(\frac{dz}{dx}\right) dxdy = \int_{-b/2}^{b/2} z_{TE} \, dy = \frac{A_{BASE}}{2}$$

Similarly

$$\sum_j S_j (\bar{x} - x_j) \epsilon_j = \bar{X} \sum_j S_j \epsilon_j - \sum_j S_j x_j \epsilon_j = \bar{X} \frac{A_{BASE}}{2} - \sum_j S_j x_j \epsilon_j$$

The summation $\Sigma\,S_j\,X_j\,\epsilon_j$ is replaced by an integral and integrated by parts, where ϵ_j is replaced by f' and f is the equation for the upper surface. Thus

$$\underset{j}{\Sigma}\,S_j\,X_j\,\epsilon_j \rightarrow \int_{-b/2}^{b/2}\int_{X_{LE}}^{X_{TE}} f'\,dx\,dy = \int_{-b/2}^{b/2} X_{TE}\,f_{TE}\,dy - \int_{-b/2}^{b/2}\int_{X_{LE}}^{X_{TE}} f\,dx\,dy$$

$$= \int_{-b/2}^{b/2} X_{TE}\,f_{TE}\,dy - \frac{V}{2}$$

where f_{LE} is assumed to be zero and V is the volume.

The remaining integral is $\overline{X}_{TE}\,A_{BASE}/2$ where $\overline{X}_{TE}$ is the distance to the centroid of the base area. Thus

$$\underset{j}{\Sigma}\,S_j\,(\overline{x}-x_j)\,\epsilon_j = (\overline{x}-\overline{x}_{TE})\,\frac{A_{BASE}}{2} + \frac{V}{2}$$

We have assumed that ϵ_j is the thickness slope in the x-z plane. Actually, ϵ_j should be the flow tangency angle. For instance, for a cone of semi-vertex angle θ_c,

$$\underset{j}{\Sigma}\,S_j\,\epsilon_j = \theta_c\,\underset{j}{\Sigma}\,S_j = \theta_c\,S = \frac{2}{\pi}\left(\frac{A_{BASE}}{2}\right) = F\left(\frac{A_{BASE}}{2}\right)$$

Similar considerations for other simple shapes indicate the deviation from our basic 2-D assumption can be corrected by introducing a factor F which is

$$F = S/(\tfrac{1}{2}\,S_{wet})$$

where S is the planform area, and S_{wet} is the wetted area of the configuration.

With the above considerations, the lift, moment, and drag equations are

$$C_L = (C_{L_\alpha})_{LT}\,\alpha\,(1 + .2\beta^{3/2}\,\alpha^2) + .6\beta\,\alpha\,(C_{L_\alpha})_{LT}\,F\,\frac{A_{BASE}}{S}$$

$$+ (.6\beta^{3/2} - 1)\,\alpha\,(C_{L_\alpha})_{LT}\,(\overline{\epsilon^2}) \tag{A14}$$

$$(C_D - C_{D_{THICK}}) = C_L \alpha + .3\beta \ \alpha^2 \ (C_{L_\alpha})_{LT} \ F \ \frac{A_{BASE}}{S}$$

$$+ \ (.6\beta^{3/2} + 1) \ \alpha^2 \ (C_{L_\alpha})_{LT} \ \overline{(\epsilon^2)}$$

$$C_M = (C_{M_\alpha})_{LT} \ \alpha (1 + .2\beta^{3/2} \ \alpha^2) + .6\beta \ \alpha (C_{L_\alpha})_{LT} \ F \ (\frac{\overline{X} - \overline{X}_{TE}}{\overline{c}} \ \frac{A_{BASE}}{S} + \frac{V}{S\overline{c}})$$

$$+ \ .6\beta^{3/2} \ \alpha (C_{L_\alpha})_{LT} \ \frac{\sum_j S_j \ (\overline{X} - X_j) \ \epsilon_j^2}{S\overline{c}}$$

and

$$\overline{(\epsilon^2)} = \frac{\sum_j S_j \ \epsilon_j^2}{S}$$

Comparisons of the ϵ^2 terms against the other terms indicate that for most configurations these terms can be neglected. However, given the details of a configuration, the contributions of these terms can be estimated.

REFERENCES

1. Woodward, F. A.; Tinoco, E. N.; and Larsen, J. W.: Analysis and Design of Supersonic Wing-Body Combinations, Including FLow Properties in the Near Field. Part I - Theory and Application. NASA CR-73106, 1967.

2. Middleton, Wilbur D.; and Carlson, Harry W.: Numerical Method of Estimating and Optimizing Supersonic Aerodynamic Characteristics of Arbitrary Planform Wings. J. Aircr., Vol. 2, No. 4, July-Aug. 1965, pp. 261-265

3. Woodward, F. A.: An Improved Method for the Aerodynamic Analysis of Wing-Body-Tail Configurations in Subsonic and Supersonic Flow. NASA CR-2228, Pts. I-II, 1973.

4. Gentry, Arvel E.: Hypersonic Arbitrary-Body Aerodynamic Computer Program (MARK III Version). Vol. I - User's Manual. Rep. DAC 61552, Vol. I (Air Force Contract Nos. F33615-67-C-1008 and F33615-67-C-1602), McDonnell Douglas Corp., Apr. 1968. (Available from DDC as AD 851 811.)

5. Carmichael, R. L.: The Prospects of Aerodynamic Performance Gains from Wing Camber and Twist at Low Hypersonic Mach Numbers. Conference on Hypersonic Aircraft Technology, NASA SP-148, 1967, pp. 79-86.

6. Sorrells, R. B., III; and Landrum, E. J.: Theoretical and Experimental Study of Twisted and Cambered Delta Wings Designed for a Mach Number of 3.5. NASA TN D-8247, Aug., 1976.

7. Handbook of Supersonic Aerodynamics, Section 7, Three-Dimensional Airfoils. NAVORD Report 1488 (Vol. 3), Aug, 1957.

8. Nelms, W. P., Jr.: Effects of Body Shape on the Aerodynamic Characteristics of an All-Body Hypersonic Aircraft Configuration at Mach Numbers from 0.65 to 10.6. NASA TN D-6821, 1972.

37

1. Report No. NASA CR-3069	2. Government Accession No.	3. Recipient's Catalog No.
4. Title and Subtitle Feasibility of Combining Linear Theory and Impact Theory Methods for the Analysis and Design of High Speed Configurations		5. Report Date December 1978
		6. Performing Organization Code
7. Author(s) D. Brooke and D. V. Vondrasek		8. Performing Organization Report No.
		10. Work Unit No.
9. Performing Organization Name and Address McDonnell Aircraft Company McDonnell Douglas Corporation St. Louis, Missouri 63166		
		11. Contract or Grant No. NAS1-15074
		13. Type of Report and Period Covered Contractor Report
12. Sponsoring Agency Name and Address National Aeronautics and Space Administration Washington, DC 20546		
		14. Sponsoring Agency Code

15. Supplementary Notes

Technical Monitor: C.L.W. Edwards (NASA/Langley)

Final Report

16. Abstract

This study examines the feasibility of combining elements of linear theory and impact theory to provide improved aerodynamic predictions for the analysis and design of high speed configurations in the Mach 4 to 8 range. Specifically, the aerodynamic influence coefficients calculated using an existing linear theory program were used to modify the pressures calculated using impact theory. Application of the combined approach to several wing-alone configurations shows that the approach gives improved predictions of the local pressures and loadings over either linear theory alone or impact theory alone. The results of the study show that the combination of linear theory and impact theory not only removes most of the shortcomings of the individual methods, as applied in the Mach 4 to 8 range, but also provides the basis for an inverse design procedure applicable to high speed configurations.

17. Key Words (Suggested by Author(s)) Aerodynamic Characteristics Aerodynamic Predictions Delta Wings Pressure Distributions High Speed Configurations	18. Distribution Statement Unclassified - unlimited
	Subject Category 02

19. Security Classif (of this report) Unclassified	20. Security Classif (of this page) Unclassified	21. No. of Pages 39	22. Price $4.50